SIAM REVIEW
Vol. 18, No. 2, April 1976

FLAGELLAR HYDRODYNAMICS*

The John von Neumann Lecture, 1975

JAMES LIGHTHILL†

Abstract. Sections 1 and 2 give a general overview of biofluiddynamic aspects of microorganisms possessing flagella and of related organisms, followed by more detailed accounts of (i) motions in eukaryotic flagellates (protozoans and algae), based on the propagation of "bends" along flagella with the characteristic "9+2" structure, (ii) motions in bacteria propelled by "bundles" of flagellar filaments of quite different structure, each driven by a "rotary motor" at its base. For analyzing all these motions, it is argued that a true "flagellar hydrodynamics" is now needed. This should replace the "flagellar dynamics" (representing the fluid medium by crude resistance coefficients) which hitherto has been universally used, but whose accuracy is insufficient for the modern microbiologist's requirements. Mathematical methods are applied to initiate the development of such a flagellar hydrodynamics in § 3. Finally, in § 4, its conclusions are summarized in nonmathematical language.

CONTENTS

1. Introduction. I am most appreciative of the honor of being selected to speak in memory of John von Neumann, and am happy to accept the invitation to survey a "significant field" or area of science where application of mathematics can yield important results. Here at Rensselaer Polytechnic Institute I gave, two years ago, a series of *ten* lectures surveying rather a wide domain of the life sciences which seemed to me to come into that general category. Those lectures were published this year by SIAM as a book, *Mathematical Biofluiddynamics.* In today's lecture, I am going to concentrate on one special field within that wide domain where the story can now be taken much further through a considerable deepening of understanding achieved during the past two years.

---

* Received by the editors June 16, 1975.

† Department of Applied Mathematics and Theoretical Physics, University of Cambridge, Silver St., Cambridge, England CB3 9EW.

Biofluiddynamics is concerned with the mechanics of the relative motions between living organisms and fluids. *External* biofluiddynamics deals with an organism's motions in relation to the dynamics of a fluid medium surrounding it, as in the study of aquatic animal locomotion or animal flight. *Internal* biofluiddynamics analyzes fluid motions inside an organism as in the study of circulation and respiration. A characteristic feature of biofluiddynamics in general is *interaction* between the motions of the fluid and of boundaries to it taking the form of highly flexible, actively motile tissue.

Within that extensive domain this lecture concentrates exclusively on one particular field: the biofluiddynamics of microorganisms. I want to give rather hurriedly a broad overview of this field as a whole, and then survey in greater depth, and in some mathematical detail, that special area within it singled out in my title, *Flagellar hydrodynamics.*

Before doing so, may I acknowledge how much I have benefited from cooperation with the interdisciplinary group of zoologists and hydrodynamicists at the California Institute of Technology studying these matters under the leadership of Charles Brokaw and Theodore Wu, respectively, as well as from similar interdisciplinary work in England bringing in many zoologists such as Michael Sleigh and Torkel Weis-Fogh, biophysicists such as Michael Holwill and Kenneth Machin, and hydrodynamicists such as John Blake, Allen Chwang and David Katz. May I also acknowledge the 1974 Caltech Symposium, "Swimming and Flying in Nature" as a most noteworthy interdisciplinary discussion, with extensive sessions on the biofluiddynamics of microorganisms, where the summary lectures by Howard Berg and by Peter Satir, on prokaryotic and eukaryotic flagella respectively, were of especial value. Finally may I thank the staff of the NERC Culture Centre of Algae and Protozoa in Cambridge for giving me such valuable help in the study of part of their magnificent collection.

The part of biology I want to concentrate on today is the part concerned with organisms at a very low level of organization into cells with differentiated functions. I am concerned to quite a major extent with organisms that are unicellular, although their reproductive cycles may involve the successive appearance of cells of various different types. I refer also to organisms in the form of aggregations of cells which may be quite large in number but which do not show any enormously greater degree of differentiation than that just mentioned.

In this respect the organisms I discuss—the protozoans, the bacteria, the algae and the fungi—are those lying at about the lowest levels of organization in the animal and plant kingdoms. These, indeed, are levels where most of the classic criteria for distinguishing between animals and plants break down, and fine gradations are observed between organisms where plant-like characteristics predominate and those where animal-like characteristics predominate, with suggestions of evolutionary developments having proceeded in *both* directions. These fine gradations of characteristics are particularly noticeable amongst the single-celled flagellate microorganisms, to which I give special attention.

On the other hand, there are more fundamental differences distinguishing the eukaryotes, or organisms whose cells incorporate membrane-bound nuclei and many other membrane-bound organelles, from the prokaryotes (including bacteria) which have no internal membrane-bound organelles. I have attempted in

Fig. 1 to give a diagrammatic guide to many interesting groups of microorganisms possessing flagella (all included within the central circle) and to related groups of organisms. The definite boundary in the form of a circular arc separating prokaryotes from eukaryotes recognizes the sharpness of that distinction.

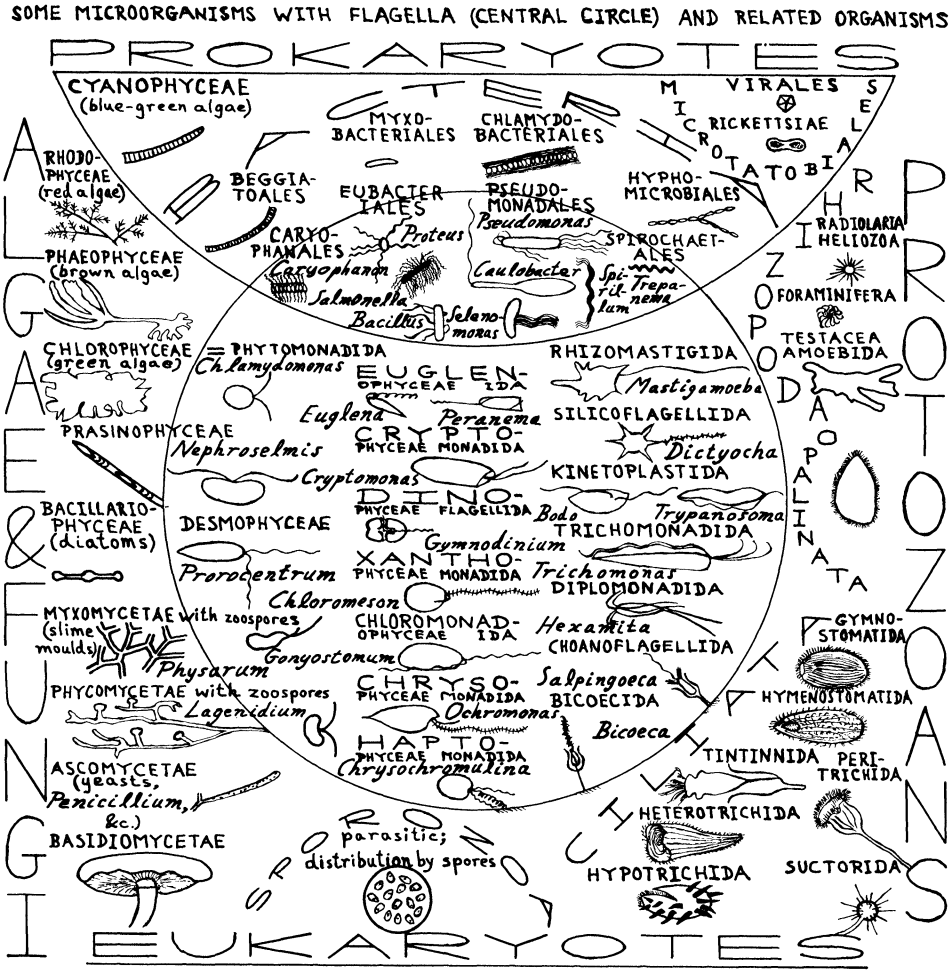

FIG. 1. *A general overview of microorganisms with flagella and related organisms*

Amongst the eukaryotes, however, there are rather fine gradations between the organisms most plant-like in character shown on the left and those most animal-like in character shown on the right. A region of overlap between spheres of interest of the botanists and the zoologists is particularly evident in the middle column, where seven different groups of organisms are noted each of which is studied by zoologists as an *order* within the flagellate protozoans and by botanists as part of a *class* of algae. Throughout Fig. 1, a class or an order is indicated in

block capitals, *under* which is usually shown a highly diagrammatic sketch of *some* species within it, in *some* stage of its life cycle. For the organisms possessing flagella (within the central circle) a partial indication of which organism has been picked out for diagrammatic representation has been given by writting the name of its genus (only) in italics. Figure 1 is used in more detail in § 2 to survey the biofluiddynamics of microorganisms possessing flagella (whether prokaryotic or eukaryotic) and of related organisms, as a background to those mathematical studies of flagellar hydrodynamics which follow. Section 2 makes brief reference also to various occurrences of similar biofluiddynamic phenomena among metazoans (so-called higher animals), of which the most obvious case is the tendency for nearly all metazoan sperm cells to be flagellate.

From a mathematical point of view, a feature common to all the biofluiddynamics of microorganisms is the overwhelming dominance of *surface* forces, such as pressure and viscous stresses, over *volume* forces such as inertial effects. In the dynamics of the fluid itself this means that fluid accelerations can be neglected and the forces on each fluid element due to pressure and viscous stress regarded as in balance. This leads to the Stokes form of hydrodynamic equations, which have the great merit of being *linear*, even though very little experience of solving them subject to conditions specified on filamentous boundaries exhibiting large-amplitude undulations has hitherto existed.

In the dynamics of a swimming organism itself, the same insignificance of inertial effects means that, at each instant, its *net swimming velocity* of translation through the fluid is determined by the following condition: this translational motion, *combined with* such undulatory motions as the organism is making, will generate *zero resultant force* on the body. This is a single 3-vector condition to determine a single 3-vector unknown: the swimming velocity.

It must be recognized, however, that even a system of force with zero resultant may have a net *moment*, setting the organism into rotation with negligible time-lag under these conditions with inertial effects insignificant. The full dynamical problem, then, is to determine a *pair* of 3-vectors: *both* a translational velocity of the organism relative to the fluid *and* an angular velocity of rotation; to determine, in other words, a general motion of the type of which a *rigid* body is capable; basically, by applying a *pair* of 3-vector *conditions*, equating to zero the net force and the net moment on the body. The organism's motile activity, in fact, is able to specify the instantaneous rate of deformation of its external surface only "to within an arbitary rigid-body movement". That movement, comprising a translation and a rotation, is uniquely determined by the requirement that the forces between the body and the fluid form a system of forces with zero resultant and zero moment.

I shall argue that flagellar *dynamics*, meaning the dynamics of organisms possessing flagella, have been worked out quite well along these lines for a variety of organisms, subject to the limitation that simple *local resistance coefficients* have been used to specify the force with which the fluid acts on a flagellum. These are coefficients of proportionality between the force acting on unit length of flagellum and its instantaneous velocity relative to the undisturbed fluid. Effectively, their use eliminates all real hydrodynamics from the problem through the fiction that the fluid resists any local movement with a local force proportional to its velocity.

It is twenty years since certain famous values for resistance coefficients for motions of a flagellum normal and tangential to itself were suggested by Gray and Hancock (1955). These are very crude representations of interaction with the fluid, suggested by known resistance coefficients for motion of a rigid cylinder. When they were introduced, they represented a very important advance, facilitating rough approximate analyses of many significant problems of flagellar dynamics; for example, relations between wave velocity and swimming speed, studies of the movements of a cell body in response to flagellar motions, estimations of flagellar rate of working for comparison with chemically determined metabolic rates, predictions of flagellar waveforms which minimize power requirements for given swimming speed, etc. Above all, they facilitated investigations of models of those presumed *internal* processes whereby an organism may generate the flagellar motions observed. Because the assumed resistance coefficients are proportional to fluid *viscosity*, models for the internal flagellar mechanics could be systematically tested by comparison of their predictions with experiments on the organism's locomotion in fluids of many different viscosities.

There are, however, many reasons why now, twenty years later, it is appropriate to initiate a true flagellar *hydrodynamics*, including analysis of the motions of the fluid medium itself. One reason is that these *fluid* motions may, for example, influence greatly the ways in which an organism either senses, or feeds from, its environment; indeed, some flagellates are sessile, with the flagella having no locomotor function but exclusively generating currents for feeding purposes. Secondly, from a mathematical point of view, it can be argued that the whole concept of local resistance coefficients is particularly inappropriate to a hydrodynamics governed by the Stokes equations, because the fundamental singular solution of *those* equations (which is the "stokeslet", representing the velocity field of a concentrated force) shows an inverse-first-power law of spatial attenuation; therefore, local forces do not produce merely local effects, but also long-range effects which need to be taken into account in studying the biofluiddynamics of a flagellate organism.

Yet another important consideration is that tentative preliminary studies of flagellar hydrodynamics, already noted in Chapter 3 of my book, suggested that any attempt at a "best possible" representation of the force distribution through resistance coefficients demands coefficients significantly greater than the Gray–Hancock values hitherto used in most studies of flagellar dynamics. Admittedly, the Gray–Hancock values were perfectly adequate for many rough approximate analyses of the general type that I just listed. After twenty years, however, the analyses where order-of-magnitude accuracy is enough have essentially been done, and the use of a more accurate representation of the force distribution has become necessary if mechanisms which energize and control flagellar motions are to be identified more precisely.

Admittedly, for much work of this kind, it will still be convenient to use the machinery of resistance coefficients. It is therefore arguable that the results of any calculations in flagellar hydrodynamics should, where possible, be given in two forms: on the one hand in terms of a "best possible representation through resistance coefficients", and on the other hand in any fuller and more accurate

manner such as may be achieved through any more complicated method of representation, possibly for use in studies of a more refined nature.

A variety of such results are given in both forms in § 3 below for a number of problems of interest. They consistently confirm the point noted above, that resistance coefficients if used should be taken significantly greater than the Gray–Hancock values, as well as giving many other suggestions relevant to the biofluiddynamics of microorganisms.

2. Biofluiddynamic aspects of microorganisms possessing flagella and of related organisms.

2.1. A general overview. Figure 1 gives a highly simplified general overview of the taxonomy of protozoans, bacteria, algae and fungi, aimed at helping those unfamiliar with that vast assemblage of organisms to find their way about the different major groupings within it. Figure 1 is also intended to draw special attention, among that vast assemblage, to the microorganisms with flagella included within the central circle.

It is worth reemphasizing the almost *continuous* gradations between plant-like and animal-like organisms illustrated in this figure. All life, of course, is founded on the activities of the autotrophic organisms: those with the characteristically plant-like ability to use various pigments to photosynthesize organic material. The omnibus expression "algae" is often used to include, *primarily*, the autotrophic (that is, photosynthetic) organisms which are at a very low level of organization into cells with differentiated functions. They range from a wide variety of single-celled organisms, through linear filamentous assemblages of cells known as trichomes, to variegated aggregations of still relatively undifferentiated cells into a much more complex thallus which as in the large seaweeeds may be very extensive. The most widely used fundamental classification of the algae is into *classes*, all of whose names end in "-phyceae", and fourteen such classes are noted in Fig. 1. From the study of some of those, however, like Euglenophyceae and Dinophyceae, we derive clear indications of how colorless organisms *lacking* photosynthetic pigments and feeding heterotrophically (that is, from absorbed organic matter) many have evolved out of autotrophic single-celled algae. For example (Leedale (1967)), the genus *Euglena* is famous for including a subgenus of such colorless algae otherwise very similar to pigmented members of the genus; and conversely, some pigmented members are able to feed heterotrophically when they are kept in the dark.

It is understandable that protozoologists, with their general interest in single-celled motile heterotrophic organisms, should have given attention to groups like these (Sleigh (1973)), assigning them in their nomenclature to a flagellate class (called Flagellata or often Mastigophora) divided into orders all of whose names end in "-ida". Some imperfect attempt at reconciliation of the algological and protozoological nomenclatures has been made in Fig. 1 (see especially the central column).

One class of algae (the blue-green Cyanophyceae) is prokaryotic: its cells lack membrane-bound organelles. The only other prokaryotes (if we put aside the viruses and rickettsiae, which of course are entirely dependent on cells of other

organisms for their growth and multiplication) are the bacteria, a very extensive class within which it is usual to place all the organisms without photosynthetic pigments; even an order like Beggiatoales whose members in many other respects are analogous to blue-green algae such as *Oscillatoria.* I should note also that one other order of bacteria (Pseudomonadales) contains not only colorless members but also a substantial minority of otherwise generally similar organisms (suborder Rhodobacteriineae) that contain certain photosynthetic pigments, though not those characteristic of the blue-green algae.

The word flagellum is used both for the filamentous attachments that confer motility on some bacteria *and* for the fundamentally different whip-like organelles that play an important role in locomotion and feeding in a vast range of eukaryotic organisms. This use of the word in two quite different senses must certainly be regretted, even though it has helped me choose a concise title for my lecture which covers just about the only feature which the two types of flagellum have in common: the associated hydrodynamics. In other respects, the bacterial flagellum is completely different from the eukaryotic flagellum, about whose structure indeed we have considerably more comprehensive information. I shall postpone to § 2.3 any discussion of bacterial locomotion, a field where many fine researches now in progress appear to be resolving some of the doubts and difficulties that have hitherto beset it, and concentrate initially on the properties of eukaryotic flagella.

No flagella are present among the the red algae Rhodophyceae, but all the other classes of eukaryotic algae (Chapman and Chapman (1973)) possess flagella of fundamentally indentical structure involving the 9 + 2 arrangement that I shall describe in more detail later, comprising 9 "doublet"-microtubules arranged in a circle around 2 central microtubules. The diameter of this circle is 0.2 μm and that of the external membrane is typically about 0.25 μm, rising to about 0.4 μm in certain flagella that carry an "intraflagellar rod" alongside the 9 + 2 structure (e.g., in euglenids). An identical morphology is found wherever flagella occur in the protozoans (Sleigh (1973)), suggesting of course that this unique 9 + 2 structure in the eukaryotic flagellum first evolved in a group of organisms that were common ancestors to all the flagellated algae and protozoans.

Outside the flagellates there are two protozoan classes—the opalinates and the true ciliates—which use the cooperative effect of large numbers of waving *cilia* for purposes of locomotion and feeding, and every one of these cilia has exactly the same 9 + 2 form and cross section as are found in a single flagellum of one of the flagellates. Finally, every flagellum or cilium occurring in metazoans possesses either the basic 9 + 2 structure or a structure obviously derived from it by some sort of "compounding" and/or reduction of central elements.

In certain classes of algae left outside the central circle, like the brown seaweeds Phaeophyceae or the diatoms Bacillariophyceae, the role of flagella is strictly limited. In the main "vegetative" phase of a brown seaweed (involving simple cell growth and cell division) they are absent. However, in this phase *sporangia* form and ultimately release reproductive cells known as zoospores, which in many of the genera are motile (through the agency of flagella rather similar to those in the zoospores of Xanthophyceae). Most diatoms in their

vegetative phase are isolated plane-symmetric cells with a characteristic hard silica wall; their normal propagation by cell division is again periodically interrupted by formation of spores that in some genera possess such flagella.

An intermediate status is represented in Fig. 1 by names shown overlapping the central circle like those of the green algae. Many of the Chlorophyceae in their vegetative phase consist of an extensive thallus, which periodically releases zoospores characterized by a pair of identical flagella emerging at the anterior end. The class, however, includes one important order, Volvocales, whose *vegetative* cells are themselves motile, appearing either as single cells as in *Chlamydomonas* or aggregated into colonies as in *Volvox*. *Chlamydomonas* swims actively with its two flagella, normally moving forwards by motions like those of the human breaststroke, though sometimes it rotates by making those motions with one flagellum only while the other remains passive. It can also be induced to beat a hasty retreat with the flagella extended while undulations pass from base to tip along them. It is hardly surprising that some zoologists have taken an interest in these particular flagellates, most of which are green, but some of which are colorless and heterotrophic, and have assigned them to a protozoan order Phytomonadida (Mackinnon and Hawes (1961)).

The related Prasinophyceae are rather more commonly single-celled flagellates with either 1, 2 or 4 flagella, although a nonmotile filamentous stage in the life cycle can occur as in *Prasinocladus*. An extreme form of the arrangement of two equal flagella emerging at the end of an axis of symmetry is seen in *Nephroselmis*, where that axis has become a short one. This organism commonly moves with both flagella undulating (Parke and Rayns (1964)).

The only kind of motility I am going to discuss in detail is that which organisms so achieve by moving one or a few flagella. Nevertheless, I shall first refer to motility of certain other kinds as of some general biofluiddynamic interest.

Certain groups of microorganisms are famous for their ability to perform a "gliding" motion along the boundary of a fluid medium. Among the Bacillariophyceae (diatoms), members of the order Pennales commonly exhibit a remarkable ability to glide, either over the smooth surface of a glass slide or even over a surface with roughnesses on the same scale as the organism itself. They seem to achieve this by exuding from a thin slit, or "raphe", a thin thread of viscoelastic mucus which, adhering to the surface, can impart a thrust to the cell sufficient to overcome hydrodynamic resistance (Harper and Harper (1967)). Similar movements, similarly associated with a viscoelastic secretion, are found in at least one family (Desmidiaceae) of green algae.

The well known movement of certain *blue-green* algae including *Oscillatoria*, which is paralleled in some of their colorless analogues (the Beggiatoales, normally placed among the bacteria), combines forward creeping at an interface with a slow transverse oscillation of the anterior end of the trichome with period a few seconds. On *Oscillatoria*, surface fibrils have been identified and tentatively implicated (Halfen and Castenholz (1970)) as a contributory influence on these gliding motions, possibly together with some kind of secretion.

Another important kind of motility in microorganisms that is affected by special rheological properties of internal fluids is cytoplasmic streaming. This is prominent throughout the protozoan class Rhizopoda, which for purposes of

locomotion and feeding depends critically on the extension and contraction of pseudopodia. The associated cytoplasmic streaming is most evident in members of the order Amoebida. The extension of their blunt or "lobose" pseudopodia with rounded ends is achieved by an internal cytoplasmic streaming which is very clearly visible. A critical role in these internal motions is played by gel-sol transitions. The continual large-scale changes of external shape play a part in both locomotion and feeding.

Although the motility of an organism such as *Amoeba* itself appears to be of a fundamentally different character from that of the flagellates, the diversity of the order Amoebida taken as a whole gives many indications of relationships to other protozoan classes. In some of the genera, organisms show various interesting responses to environmental changes: for example, to lack of moisture by forming a spherical, strongly walled cyst within which the organism remains inert until the environment becomes more moist; or conversely responding to a major dilution of the liquid environment by growing some flagella which may proceed to propel the organism away from its nutrient-deficient location (Mackinnon and Hawes (1961, p. 26)). Some other organisms (Rhizomastigida) may execute amoeboid movement and yet possess a permanent flagellum; those perhaps lie almost on the boundary between rhizopods and flagellates, but from the points of view of Fig. 1 must clearly be placed within the central circle. For example, *Mastigamoeba*, besides exhibiting cytoplasmic streaming, often pulls itself forward by undulations passing along its flagellum from tip to base (Sleigh (1973, p. 36)).

Within parasitic genera of Amoebida, certain species form a cyst within which cell division takes place. This forms a link with the extensive protozoan class Sporozoa, where a spherical cyst within which spore formation occurs is normally an important stage in the life cycle, but this class of parasitic organisms will not figure significantly in the present survey, owing to its restricted degree of biofluiddynamic interest.

A certain degree of cytoplasmic streaming is readily observed in some of the flagellates proper, including many of the Euglenida; in those it produces definite and substantial fluctuations of shape, although they are not nearly so marked as in *Amoeba*, and the dominant motile role is played by the flagella. A similar combination of two kinds of biofluiddynamic interest is exhibited by the slime moulds, usually studied (Smith (1955)) as a botanical class Myxomycetae remotely related to the fungi proper, but occasionally described as a rhizopod order (Mycetozoia) by protozoologists. The vegetative phase exhibits very marked cytoplasmic streaming, often in an exceedingly "naked" form with regularly reversing flow taking place in the branches of an intricate open network known as a plasmodium. Ultimately one or more sporangia are formed from which there emerge zoospores which are amoeboid in some genera but flagellate in others (such as *Physarum*).

The fungi proper are far more definitely plant-like in character (Smith (1955)) except, of course, that they also are entirely heterotrophic. Members of the class Phycomycetae (often called the "lower" fungi) generate a wide range of different types of spore, *including* flagellated zoospores with either one or two flagella. "Higher" fungi have much more distinctive types of spore, without flagella, although in the case of the Basidiomycetae we find that dispersion of the

species is often achieved by a different kind of spore locomotion: the basidium, through a mechanism that remains obscure, acts as a gun which explosively expels the spore, at a speed far exceeding the terminal velocity of these light objects. Accordingly, the trajectory is practically two straight lines (one followed by the spore in the direction of discharge till its momentum is almost spent, and one vertically downwards with the terminal velocity)—a trajectory so different from the familiar parabola characteristic of heavy objects that one mycologist christened it the "sporobola"!

Returning to the rhizopod protozoans, we must note that their pseudopodia instead of being lobose as in most of the Amoebida may often take fine filamentous forms (which need of course to be sharply distinguished from flagella). The Testacea are amoeboid organisms living in a sort of shell or "test", from openings in which they extrude pseudopodia of *either* lobose *or* filamentous form; but the especially famous and abundant order of shelled protozoans is the Foraminifera, with their variously "sculpted" shells from which a network or reticulum of filamentous pseudopodia emerge for purposes of feeding. Some Foraminifera use the reticulum also for locomotion to pull themselves along some surface such as that of a seaweed (Mackinnon and Hawes (1961, p. 51)).

An especially interesting filamentous pseudopodium is the *axopodium* found in Heliozoa and some Radiolaria. The organisms are typically spherical floating protozoans, from which emerge axopodia, each possessing an axial skeletal element that allows them to remain rigid. The skeletal element is commonly formed by means of an arrangement of microtubules, which however, is geometrically quite different from that found in flagella and involves a much greater number of separate microtubules. Feeding often proceeds through partial withdrawal of one or more axopodia to which food particles have adhered. In addition, heliozoans have been observed moving over a solid surface by a rolling mechanism (Sleigh (1973, p. 161)) brought about by cyclic extension and withdrawal of the axopodia.

The last biofluiddynamic topic that I wish to touch upon briefly before focusing attention on flagellar hydrodynamics proper is the role played in locomotion and feeding of ciliates by the cooperative action of large members of waving cilia. I mentioned that cilia have the same *internal* structure as flagella, but of course their hydrodynamics is quite different because it depends on the statistical effect of the very large number of organelles involved.

We can quickly pass over the small isolated class Opalinata with only four genera, all found in frogs' guts and all of which except in the possession of cilia are completely different from the true ciliates. In particular, they lack a mouth and take only liquid food through the cell membrane. They do possess more than one nucleus but are without the big macronuclei found in ciliates. Their methods of multiplication are also quite different, involving on the one hand cell divisions of a very simple kind, and on the other hand a cyst stage for the part of the life cycle spent outside the host. Finally, their locomotion is different: the cilia remain very close together while a wave of movement passes over them like the undulation of a field of corn, the animal progressing slowly in the opposite direction to the wave. Both observation and hydrodynamic analysis indicate (Blake and Sleigh (1974)) that this method of organizing ciliary locomotion *through a fluid* generates speeds

less by an order of magnitude than the method mainly used by true ciliates; but possibly for opalinates in the rectum of a frog it may be more important that the motions are effective in a *crawling* mode, with the cilia beating against the gut wall, so as to avoid elimination when the frog defecates!

True ciliates are animals far more complex in several different ways (Sleigh (1973)). They exhibit a specialized type of binary fission at an equatorial plane involving replication of the whole ciliate's intricate structure. This is sometimes preceded by the unique sexual process of *conjugation* where two cells are closely juxtaposed and one of the two gamete nuclei in each is passed to the other cell across a cytoplasmic bridge. Only the ordinary nuclei (or "micronuclei") take part in the sexual process, which is preceded by the disintegration of the one or more big macronuclei (which are involved only with the various metabolic functions of the cell). The daughter cells then proceed to reconstitute the numbers of macro- and micronuclei characteristic of the species.

Each cilium arises from a "basal granule" or "kinetosome", and the cilia are typically arranged in rows called kineties. They are important both for locomotion and feeding, with the relative importance varying in different groups of ciliates. They are primarily important for locomotion in the Gymnostomatida, which have no specialized mouth ciliature and where cilia are distributed uniformly over the surface, although with kineties converging towards the general mouth area. Motions of somatic cilia of this general type have been particularly studied in the Hymenostomatida (e.g., *Tetrahymena* and *Paramecium*), where they are found along with *some* specialized mouth ciliature. Each somatic cilium makes its effective stroke in a condition of temporary separation from adjacent cilia, as a nearly rigid rotation about the base pushing fluid along the body surface in a direction opposite to that of locomotion. The recovery stroke takes place in a different plane, almost tangential to the surface, again with the cilium almost rigid (much *more* so than was formerly believed from observations made at right angles to the kineties). The wave of motions is "dexioplectic" in the sense that it passes spirally forwards and to the *right* (Machemer (1972), Sleigh (1974)); it is this organization of the motions which avoids interference between the actions of adjacent cilia. As a result, an organism 0.25 mm long may move at speeds of 1 to 2 mms^{-1}.

Specialized mouth ciliature may include (i) a group of cilia essentially coalesced to form an *undulating membrane* generating a flow of fluid bearing suspended food particles towards the mouth cavity, and (ii) a complex structure known as the AZM (adoral zone membranellae), where again each membranella consists of many cilia more or less adhering to one another. In Fig. 1, four of the orders in the subclass Spirotricha (Mackinnon and Hawes (1961), Sleigh (1973)) are mentioned, with some illustration of the prominent spiral arrangement of the AZM which facilitates feeding (and usually locomotion as well) by a biofluid-dynamically interesting propeller-like action of considerable vigor. A few of these like *Stentor* in the Heterotrichida retain somatic ciliature but most commonly this is lost, or else replaced as in the Hypotrichida by *cirri*, each of which is a bundle of numerous adhering cilia that wave as one.

Contractility of the cell body, acting as an important defense mechanism, is found in many members of this subclass, including *Stentor*; and similarly the

elegant *Tintinnopsis campanula* is able to contract its cell into the relatively rigid "lorica". Certain members of the order Peritrichida like *Vorticella* are at most times sessile, using the ciliature *only* for feeding, and are famous for the exceptionally rapid contractility of the stalk or "spasmoneme".

I will now terminate this extremely brief look at a few ciliate orders by mentioning the aberrant Suctorida, which in the adult stage lack cilia together! However, in other ways they are like ciliates: they possess macro- as well as micronuclei and exhibit conjugation, normally between two neighboring sessile animals, and furthermore do produce larvae that use somatic cilia to swim to find a new attachment site. Possibly a certain degree of biofluiddynamic interest is afforded by the hollow tentacles of adult Suctorida such as *Discophrya* which can exert a powerful suction effect, holding on to some prey, puncturing its cell membrane and sucking out its contents.

2.2. Eukaryotic flagellar motions. Now it is necessary to consider flagellar motions in more detail. Several times I have mentioned *undulations* in a eukaryotic flagellum. It is important to recognize that these take place without any changes in its cross-sectional dimensions, which are fixed by the geometry of the $9 + 2$ microtubules. Similarly, there is no *stretching* of the flagellum, or indeed even of the individual microtubules. We shall see later that to form a *bend* the microtubules on the outside of the bend make "walking" movements on the little "limbs" by which they are attached to neighboring microtubules, and conversely the microtubules on the inside of the bend make opposite walking movements, generating a bend through this active shear in the plane of the bend fitting in a greater length of (unstretched) microtubule on the outside of the bend opposite a smaller length of (unstretched) microtubule on the inside of the bend.

Undulations, then, take place in an effectively inextensible flagellum and so can only take the form of transverse waves, similar in *appearance* to those which can be passed along a rope by shaking one end, even though, of course, quite different mechanisms for generating the waves operate in the two cases. Now, the classical paradox of a transverse undulation passing along a rope (say from left to right) is that although at every point there is always an appearance of something moving to the right, no net displacement to the right occurs. The explanation of the illusion is, of course, that the eye is sensitive to motions of the rope normal to itself but not to tangential motions. The *normal resultant* of the velocity of a particle of rope has always a left-to-right component, as the eye observes. Accordingly, the *average* normal resultant points from left to right. Evidently, to balance that, there must be an exactly equal and opposite average *tangential* resultant, pointing from right to left, equal and opposite because the tangential and normal resultant add up to the total velocity of a particle of rope, whose average is zero.

An undulation, then, as it propagates along any flagellum attached to a cell body, generates average *normal* motions relative to that body which are in the direction of propagation. These are accompanied by equal, and oppositely directed, average *tangential* motions.

With this background we can readily appreciate the significance of local resistance coefficients which may be so *anisotropic* that the fluid resists normal

motions of a small length of smooth flagellum with a force almost double that with which it resists equal tangential motions. This law of Gray and Hancock, which has a crude approximate validity even though I will seek to refine it in § 3, implies that the average fluid forces opposing normal motions (which are in the direction of propagation, relative to the cell body) are almost double those acting to resist the equal and opposite tangential motions. The difference is a net thrust, opposite to the direction of propagation, for such a smooth flagellum.

Evidently this net thrust generates a motion of the organism as a whole in a direction opposite to the direction of propagation at such a speed that the resistance to that motion just balances the thrust. In this way *Mastigamoeba*, as we saw, is pulled forwards by the undulations passing along an anterior flagellum from tip to base, whereas a dinoflagellate like *Gymnodinium* is pushed forwards by undulations passing along a posterior flagellum from base to tip.

It has long been recognized that the above argument goes into reverse for an organism which propagates a planar waveform along a flagellum with projecting *mastigonemes* in the plane of the undulation (Holwill and Sleigh (1967)). Mastigonemes are "hairs" about 1 μm long and 0.02 μm thick projecting on both sides of the flagellum of (say) a chrysophycean like *Ochromonas* or a xanthophycean zoospore. They remain stiff during its motion (Holwill (1974)). Such mastigonemes, when the flagellum moves in their own plane, make the coefficient of resistance significantly greater for tangential motions than for normal motions. Therefore, planar undulations of this type of flagellum generate a thrust *in the direction of propagation*, and indeed the organisms are observed to pull themselves forwards by propagating such a wave *from base to tip.*

Most algologists and protozoologists make a distinction between, on the one hand, flagella bearing true mastigonemes thus stiffly projecting on both sides roughly at right angles, with the apparent function of changing the relative values of tangential and normal resistance coefficients in planar motions, and on the other hand flagella as in *Euglena* exhibiting much flimsier tinsel-like hairs, usually on one side only. (The German word for tinsel, "Flimmer", is, however, often used to describe either type of flagellar projection.) These much flimsier attachments (not illustrated in Fig. 1) are likely, particularly in spiral motions characteristics of euglenid flagella, to produce comparable small increases in *both* the normal and tangential resistance coefficients and therefore to give basically the same dynamic properties as a smooth flagellum (if anything, a little enhanced). Neglecting those refinements, together with any similar effects of scales covering the flagella in, for example, the Prasinophyceae (Chapman and Chapman (1973, p. 28)), I propose to discuss the observed motions of all such organisms in what follows from the simplified standpoint of smooth-flagellum analysis.

I want to emphasize that my earlier explanations of why a wave propagated along a smooth flagellum generates a thrust in a direction opposite to that of propagation are valid *both* for planar waveforms of any shape (whether sinusoidal or otherwise...) and *also* for three-dimensional waveforms such as spirals. It is worth noting that planar waveforms have the disadvantage that the thrust they generate is *spatially inhomogeneous*, being significantly positive in those parts of the wave where the normal resultant is greatest because they are inclined substantially to the direction of propagation, while actually becoming negative

(though small in magnitude) in parts nearly parallel to that direction. We shall see that such spatial inhomogeneity increases the energy cost required to produce a given net thrust.

By contrast, a spiral waveform, that has all parts equally inclined to the direction of propagation, can generate thrust homogeneously, with a significant reduction in the total energy cost required to produce given thrust. On the other hand, the forces generated by a spiral wave in a single flagellum combine to give not only a resultant thrust but also a resultant moment about the axis of the spiral. The net effect is that not only does the organism as a whole move in the direction of the thrust, but also the cell body has to rotate, at such an angular velocity that the couple opposing its rotation balances that generated by the spiral undulation (Chwang and Wu (1971)). This rotation of the cell body must produce some additional energy dissipation; nevertheless, the fatter the cell, the more readily it can generate this opposing couple with a relatively slow rotation and therefore a relatively small additional energy dissipation.

Thus, propagation of a spiral waveform along a single flagellum generates thrust efficiently, but it generates also a couple that causes the cell body to rotate at some additional energy cost. Note also this rotation of the body is likely to generate an equal rotation in any flagellum attached to it. This can have two alternative possible drawbacks: if on the one hand the cell body's own motions are simply added on (as rigid body rotations) to the motions of the spiral, they give it a supplementary corkscrew motion which generates a force *opposing* the thrust due to the undulation (so that the net thrust is reduced). On the other hand, a kinematically possible alternative mechanism which has been suggested in another context (Wang and Jahn (1972)) is *flagellar self-rotation*, whereby the whole length of the spiral flagellum generates active shearing movements that allow it to avoid normal displacements and merely twist everywhere about its own *curved* axis, but this solution would bring its own internal metabolic costs and control complexities.

It hardly appears fanciful to see in the special morphological features of many flagellates (Fig. 1) a series of methods of reaping the advantages of spiral-wave propagation without the disadvantages. Evidently flagella like those of *Chlamydomonas*, which are "isokont", that is, equal and symmetrical, can avoid generating any couple whenever they beat symmetrically. Many other biflagellate organisms possess, on the other hand, a main propulsive flagellum and a subsidiary flagellum whose functions may well include control of rotation about the antero-posterior axis. For example, in a dinoflagellate like *Gymnodinium*, this is the transverse flagellum which undulates in a transverse groove to generate a couple about that axis. Similarly, in the Desmophyceae, a subsidiary flagellum makes a relatively slow beat while the propulsive flagellum pulls the organism forwards by means of a fast tip-to-base undulation (Chapman and Chapman (1973, p. 148)).

Some support of the proposition that the transverse flagellum in Dinoflagellida may have a role in increasing thrust through control of rotation is provided by an important observation of Jahn, Harmon and Landman (1963) on *Ceratium tripos*. Admittedly, they noted that the posterior flagellum often makes planar undulations; nevertheless it is very likely that it can additionally propagate a

helical wave to generate fast motions. Jahn et al. (1963, p. 360) observed that the organism's substantial rotation (as viewed along its direction of locomotion) was anticlockwise or clockwise *according as the transverse flagellum was or was not beating.* This strongly suggests that (i) with inert transverse flagellum, the posterior flagellum propagates a helical wave generating a *clockwise* rotation of the cell body, which in turn produces an additional corkscrew motion of the helix that reduces its net thrust; whereas (ii) the beating of the transverse flagellum can reverse that rotation, adding an *anticlockwise* corkscrew motion to the flagellum and so actually *increasing* its thrust.

In *Euglena* the interesting and superficially awkward arrangement of its one effective flagellum may have even more subtly turned what is potentially the main disadvantage of spiral undulations into an advantage. *Euglena* exhibits very clearly those body rotations which (as usual) are necessitated by the unbalanced couple due to the spiral undulation of its flagellum. When it moves forwards, with the flagellum characteristically trailing from the anterior end (and giving thrust by a base-to-tip spiral undulation), it seems inevitable that these rotations of the body must be transmitted past the 180° bend. (All the indications are that the 9 + 2 structure is unable to sustain the high local torsion that would otherwise be required.) But a rotation in being transmitted by the torsional stiffness of a flexible filament around a 180° bend *reverses the sense of its rotation in space.* If the resulting reversed rotation simply adds to the spiral undulation a rigid corkscrew motion, this accordingly has now the right sign to *add* to its propulsive thrust—a really useful bonus from the extra rate of energy expenditure required for body rotation! This mechanism requires only a minimal amount of active shearing (confined to a cyclic active shear in the 180° bend itself at the frequency of body rotation)—far less than is required by the hypothesis of general flagellar self-rotation.

From among the considerable diversity of modes of locomotion found in other euglenids, I pick out those of *Peranema,* a colorless organism that ingests particulate food through its mouth-like cytostome. Its anterior flagellum is thickened (like that of *Euglena*) by the presence of an "intraflagellar rod" alongside the 9 + 2 structure. It swims in a spectacular manner with this flagellum stretched forwards; the posterior half remains almost motionless, while a very energetic propulsive spiraling proceeds at the anterior end. The body is observed to turn in response to the resulting couple but (probably owing to its fatness) the angular velocity of turn is slow enough to reduce only slightly the propulsive effect of the spiral undulation. (There is a thin posterior flagellum, which is observed to adhere closely to the cell; this is unlikely to have a rotation-controlling function since any couple which it generated in forward motion would be small owing to the proximity of the cell body.) *Peranema* is additionally able, at an interface, to execute a gliding motion (associated like that of diatoms with a viscoelastic secretion) with the anterior flagellum straight except for quite a slow movement at the tips (Chen (1950)).

The Cryptophyceae are a not so well-known group of single-celled organisms that may be pigmented or colorless. They have a rather characteristic asymmetrical form and two slightly unequal tinsel-like flagella, whose motions it would be interesting to record and analyze. Members of the genus *Cryptomonas* are green

and may be observed moving in rather a versatile manner in cultures, either forwards or backwards and usually slowly rotating about the antero-posterior axis.

The Xanthophyceae are a class of pigmented algae (usually yellow-green) where the vegetative phase may involve various colonial aggregations and filament-like or sac-like forms or may consist of single cells. Such a vegetative single-cell may be flagellate, or else amoeboid, or even capable of alternating between the two forms. All the Xanthophyceae, however, form flagellated zoospores, which typically swim around quite fast. The longer of their two unequal flagella bears mastigonemes and propels the zoospore with a planar undulation just as in *Ochromonas.*

The Chloromonadophyceae are a small class with pigmented and nonpigmented members, all single-celled (Chapman and Chapman (1973, p. 140)). They show a certain amount of cytoplasmic movement even in their typical biflagellate state (the cells may also repond to environmental changes by adopting amoeboid or encysted forms). In locomotion, one of the two flagella trails and could possibly have a rotation-controlling function.

The Chrysophyceae are a large class, including many single-celled forms, mostly pigmented (yellow to golden-brown) but some colorless, together with a variety of colonial aggregations and branched-filament forms. Both in typical single-celled forms like *Ochromonas* and in typical zoospores of multicellular forms, there is a propulsive flagellum with mastigonemes *and* (sometimes) an additional short smooth flagellum (however, both isokont and rhizopod forms are known). *Ochromonas,* as we saw earlier, swims forward with a base-to-tip planar undulation. Algologists normally include among the Chrysophyceae the identically pigmented single-celled uniflagellates with an internal siliceous skeleton that some zoologists have assigned to an order Silicoflagellida. They have slender pseudopodia and a flagellum with mastigonemes, presumably executing a similar planar undulation.

I want to refer next to a wide variety of organisms each of which is sessile for a significant part of its life cycle, during which, however, it continues to make very active flagellar movements. These are organisms where the locomotor function of flagellar movements may go into abeyance but the feeding function remains. Often the cell is attached to an inert cup-shaped lorica.

One famous pigmented chrysophycean *Dinobryon* secretes such a lorica to which it remains attached by a contractile cytoplasmic "stalk". A daughter cell often builds its lorica on the mouth of an empty old one, generating a colony of tree-like appearance. *Dinobryon* is often found (Sleigh (1973, p. 264)) in waters that are oligotrophic (deficient in salts needed for algal growth) and the continual activity of its flagella (broadly like those of Ochromonas) may be important for maintenance of its salt intake by ensuring a steady relative flow of fluid past the colony.

The Bicoecida, a group of heterotrophic flagellates usually classified as a protozoan order, may have evolved from colorless derivatives of such loricate chrysophyceans. *Bicoeca* uses its secondary flagellum to attach the cell to the lorica which it has secreted (and which in turn is usually attached to some substrate). The primary flagellum with its mastigonemes performs a vigorous base-to-tip undulation (Sleigh (1973, p. 122)), but the thrust it generates (also

directed from base to tip, because of the mastigonemes) is balanced by the tension in the secondary flagellum. Opposed to that thrust, however, is an equal reaction force on the *water*, which causes it and any food particles suspended in it to stream continuously towards the organism, which ingests particles by means of pseudopodia.

Rather a different structure is exhibited by Choanoflagellida, possessing only a single flagellum with which they exert a thrust in the opposite direction—*into* the lorica, for example, in *Salpingoeca*. The reaction on the water is then to force it away from the cell; part of this water current is filtered by the "collar" of fine pseudopodia which trap and ingest food particles suspended in it. Some other genera of these "collar-flagellates" form small colonies (Sleigh (1973, p. 121)).

One special reason why this order is interesting derives from the fact that the mechanically active elements in *sponges* (members of the phylum Porifera, at the next level of animal organization into cells with differentiated functions above the Protozoa) are the "flagellated chambers" made up of "choanocytes", cells fundamentally similar to those of the Choanoflagellida. The skeleton of the sponge provides support for a complicated ducting system giving access of water to numerous different flagellated chambers where the pumping activity of the choanocytes ensures a steady through-flow and the capture of food particles by the filtering action of the collars (see, for example, Hyman (1940, pp. 284–364)).

Another remarkable group of single-celled flagellates, some with capabilities of attachment to a substrate, are the Haptophyceae. They possess a pair of isokont flagella like *Chlamydomonas* and they also possess a third fibrillar organelle which is not a flagellum and indeed never exhibits flagellar beating movements or undulations. This is the "haptonema" with its unique structure of microtubules (characteristically 7 instead of the 9 + 2 in a flagellum) and its capacity for coiling and uncoiling (Sleigh (1973, p. 32)). *Chrysochromulina* sometimes makes free swimming movements like *Chlamydomonas,* either with breaststroke-like motions of its two flagella or with undulations, and with the haptonema either held out rigidly in front or else trailing. Alternatively, it uses the haptonema to attach itself to a substrate while the flagella continue to beat vigorously. The resulting water currents may assist in feeding because, although the organism photosynthesizes, it also ingests food particles at the pole opposite to the point of attachment (Chapman and Chapman (1973, p. 172)).

There is in the flagellates just one more special type of structure that I should like to describe because of its definite biofluiddynamic interest. This is found in *Trypanosoma*, an extensive genus of organisms with complicated life cycles (Mackinnon and Hawes (1961, p. 117)), some members of which are notoriously dangerous to man. It is the bloodstream form (trypomastigote) of *Trypanosoma* that characteristically exhibits an "undulating membrane". This is a *true* membrane, continuous with the cell membrane *and* with the membrane around the axoneme (9 + 2 structure), and thus is quite different from the so-called undulating membrane in ciliates (made up of a mass of more or less adhering cilia). When the axoneme undulates, a wave passes down the whole undulating membrane, with very marked propulsive effect.

The same phenomenon is found in *Trichomonas*, an organism that possesses also an interior skeletal rod (axostyle) and three anterior flagella. In this lecture,

however, I shall not try to analyze these complex motions, or those of flagellates possessing great numbers of flagella. *Hexamita* was named when it was believed to have six, but in fact has eight, and others (in the order Hypermastigida) may have hundreds (Mackinnon and Hawes (1961, p. 138)). It is probably from flagellates of such a type that the true ciliates evolved.

2.3. Bacterial flagellar motions. I return now to the locomotion of bacteria, and to the character of those filamentous attachments commonly associated with their locomotion which are called "bacterial flagella" even though they differ fundamentally from eukaryotic flagella in all save perhaps a few hydrodynamic aspects! I shall discuss primarily locomotion associated with the movements of such bacterial flagella, although referring also to bacterial locomotion associated with analogous movements of a cell body. I shall say no more about those orders of bacteria which apart from being colorless appear quite closely related to blue-green algae (including Beggiatoales, with their cells arranged in filamentous "trichomes" capable of a gliding motion as already discussed, Chlamydobacteriales, with trichomes enclosed in sheaths, and perhaps Hyphomicrobiales, with branching filaments) but I will in passing mention a different gliding phenomenon exhibited by the single-celled flexible elongated Myxobacteriales at an interface (Weibull (1960)). This gliding motion is ascribed by some authors to yet another viscoelastic secretion, but by some to a sort of worm-like creeping.

The names of two exceedingly large orders of bacteria are placed at the top of the central circle in Fig. 1: Eubacteriales and Pseudomonadales. Each is shown *overlapping* the boundary of that circle because, while each order contains a vast number of members with flagella (of which a few are illustrated), each also contains a very large number of nonmotile members (including in particular almost all the organisms of "coccus" shape—spherical or spheroidal).

The types of flagellar arrangement found in those members of the two orders which are motile are, however, quite different (Salle (1961)). In the variously shaped Pseudomonadales, all flagella are "polar" in the sense that they emerge from one or both ends of some axis through the organism. At each "pole" there may emerge either no flagella, or one, or a few, or many, but there are no other locations where flagella emerge. By contrast, motile members of the Eubacteriales, which are usually rod-shaped, have flagella that are "peritrichous" in the sense that they arise (whether in moderate number as in *Proteus mirabilis* or in large number as in *Salmonella typhosa*) from locations all around the cell body.

It must be emphasized that the difficulties of obtaining data on locomotion are enormously greater for bacteria than for eukaryotic flagellates because dimensions are less by an order of magnitude. A bacterial cell has typical dimensions of order 1 to 3 μm (in the region where Brownian motion is significant), as compared with values of order 10 to 30 μm for typical flagellates (and much larger values still for many euglenids and dinoflagellates). The thickness of a bacterial flagellum is of order 0.02 μm, as against 0.2 μm for the eukaryotic 9 + 2 structure even without its enveloping membrane. Crudely, we can say that all dimensions are down by an order of magnitude, producing many general difficulties in studying the motions and the particular difficulty that the

individual bacterial flagellum cannot normally be resolved with the light microscope.

Admittedly there have existed for many years various ingenious techniques for "staining" the bacterium and its flagella in such a way that photomicrographs showing the shapes of the flagella (as thickened by the stain) could be obtained. More recently, electron micrography enormously increased the quantity of anatomical data available. There is, however, a grave lack of techniques for obtaining detailed kinematical information on the motions of bacterial flagella. Only in the last 2 years has it become possible, from many fragmentary indications, to piece together a picture that begins to appear self-consistent.

In the organisms with around six peritrichous flagella (*Proteus mirabilis* or *Bacillus megaterium* or the well-known *Escherichia coli*, on which much of the research work has been done), the types of gross motion of the cell as a whole that it is necessary to account for are as follows (see, for example, Berg and Brown (1972)). The bacterium performs something like the mathematician's idealized concept of a "random walk": it alternates "runs" and "twiddles" (also called "tumbling"). The "run" is a period of approximate motions in a straight line, pushed by the activity of a "bundle" of flagella behind it. This bundle involving all of the flagella, forced close together by hydrodynamic (and possibly also other) forces, scatters enough light to be visible against a dark field. The "twiddle" (or "tumble") involves a random change of direction: for one brief instant the flagella are not aggregated together; then the bacterium makes another "run" in a new direction with them gathered behind it in a propulsive "flagellar bundle" once more.

The behavioral reaction called "chemotaxis" whereby a bacterium statistically tends to go *up* any gradient of one category of solvents called "attractants", but to go *down* any gradient of another category of solvents called "repellents", has been shown to be generated by a variation in the *frequency* of "twiddles". Essentially the organism makes those sudden changes of direction *less* frequently when its chemoreceptors sense an increasing concentration of attractant (or a decreasing concentration of repellent), whereas it twiddles *more* frequently on sensing a decreasing concentration of attractant (or an increasing concentration of repellent). Crudely speaking, it observes the following strategy: when things are improving, "keep going", and otherwise "look around".

Recent work by Macnab and Koshland (1974), extending earlier work there referred to, demonstrated that a very high intensity of light in a certain (blue) part of the spectrum acted as a repellent in the sense that it increased the frequency of twiddles reversibly. This work should not be confused with the classical phenomenon of "phototaxis"—the light-seeking response observed in many of the photosynthesizing bacteria. The new experiment, carried out on a species of *Salmonella*, used an arc lamp of very high intensity with various filters including a yellow filter that was briefly removed generating more frequent twiddles and replaced restoring the normal frequency.

A very interesting by-product of this use of illumination of exceptionally high intensity was the greatly improved visibility achievable in oil-immersion dark-field microscopy. This confirmed very clearly the general impression of previous

authors that the flagellar bundle forms a left-handed helix, the same shape as a stationary flagellum is shown to have under the electron microscope. Furthermore, in this experiment the individual flagella could be momentarily distinguished during a "twiddle" as temporarily separated from one another.

It has long been recognized that a flagellar bundle in the shape of a left-handed helix may propel a bacterium in one of two ways: *either* it may be given a clockwise rigid rotation (or nearly rigid rotation) like a corkscrew from its base inside the cell wall, *or* it may propagate a wave from base to tip just like a eukaryotic flagellum. In either case, the moment on the helix must be balanced by a moderate anticlockwise rotation of the cell body; this *either* reduces the rotational velocity of the flagellar corkscrew relative to the water by around 20% *or* else makes a similar reduction in the propulsive thrust of the spiral wave by adding on an opposing corkscrew-like rotation. Observations show, indeed, just such a counterbalancing rotation of the cell body (anticlockwise as seen looking backwards along the flagellar bundle). This supports the view that one of those two mechanisms is responsible but gives no help in distinguishing between them.

At first sight, the theory that the base region of each bacterial flagellum "contains a rotary bearing and motor" that can generate a continuous rotation of the flagellum relative to the cell body (at around 10 to 20 revolutions per second) seems "unbiological", mainly because no such system was ever developed in the vast range of different types of locomotion achieved by eukaryotes (though admittedly the evolutionary pressures on the bacteria in their quite different range of sizes were quite different). Recently, however, the weight of evidence supporting the idea of a rotary motor has begun to appear very strong indeed.

One way of distinguishing a bundle of rods that are all separately rotating from a different situation involving *turning of the bundle as a whole* (as the spiral-wave hypothesis requires for the flagellar bundle) is that tying together two points on different rods stops them from rotating independently but does not prevent turning of the bundle as a whole. Now, many antibodies are known that attach themselves selectively to the flagella of *Escherichia coli*; some are monovalent (attaching themselves at a single site) and some are divalent. Normally a divalent antibody will attach itself to two sites on one and the same flagellum, when its effect on restricting the motility of the bacterium should be no greater than in the monovalent case; but there is a certain small probability that it may attach itself at sites on two separate flagella, tending to tie them together. It was interesting, therefore, that the concentration of antibody required to remove the motility of half the bacteria in the sample was *two orders of magnitude lower* for divalent than for monovalent antibodies, tending (Berg and Anderson (1973)) to support the theory of separate rotation. More recently, polystyrene latex beads 0.7 μm in diameter have been attached to bacterial flagella and observed (Silverman and Simon (1974)) to rotate in the opposite sense to the cell body, in further support of the theory.

It is necessary at this stage to recall that a bacterium has all of its cytoplasm surrounded by a "cytoplasmic membrane", which in turn is surrounded by a separate "cell wall". It has long been known that a flagellum emerges through a hole in the cell wall from a "base area" associated with the cytoplasmic membrane. In several species, base areas of disc-like character have been identified.

The rotary motor could be the result of a continuously active shearing process between such a disc and the cell wall (Berg and Anderson (1973), Berg (1974)). We shall see later that this is indeed a more plausible location for processes converting chemical into mechanical energy than is the exceedingly restricted cross section of the flagellar filament itself.

On the rotary hypothesis, the "twiddle" is regarded as a brief period when some of the rotary motors go into reverse, causing the bundle to fly apart as different flagella are subjected to opposing forces. When all are rotating in the same sense once more, the bundle tends to form up along some different direction.

Before going into more detail on mechanisms, I want to indicate something of the diversity of bacterial motions that are found. Among bacteria with peritrichous flagella, cooperative motions by a large number of individual bacteria are sometimes observed, as when a colony of *Bacillus alvei*, half a millimeter in diameter, moved a distance of over a centimeter in one hour (Salle (1961, p. 93)) during which the colony continued to keep together. Again, the order Caryophanales includes three interesting genera *Caryophanon*, *Lineola* and *Oscillospira* consisting of long trichomes (as much as 30 μm in length) of actively motile pertrichous bacteria. Cooperative motions would repay study from the standpoint of the rotary hypothesis.

Among the Pseudomonadales with polar flagella there is beginning to emerge a considerable amount of evidence to support the rotary hypothesis, even in a *Pseudomonas* species (*cirronellosis*) that is monotrichous (with one flagellum only). In that species the flagellum is again a left-handed helix (Taylor and Koshland (1974)) which pushes the cell body by rotation which is clockwise (looking along the flagellum from its base). Rotation is reversed for brief periods (corresponding to tumbling in a peritrichous bacterium) during which the organism briefly retreats before making the next advance. Again, the stalked bacterium *Caulobacter* is monotrichous, pushing itself by the action of the flagellum at one end of the stalk during its motile phase before using the stalk to attach itself to a substrate (Salle (1961, p. 410)).

Other species of *Pseudomonas* have a greater number of polar flagella operating in a bundle. With the Pseudomonadales generally the small polar areas of the cytoplasmic membrane which include the points of origin of all the flagella have structures that are recognizably different from the rest of the membrane and may well be associated with generating flagellar rotation. This is true both of the only such area in *Selenomonas*, which includes the origins of around 20 different flagella (Kingsley and Hoeniger (1973)), and of the two polar areas in *Spirillum* each with several flagella attached to it (Smith and Koffler (1971, p. 226)).

Spirillum is an unusual genus in many ways: the cell is much longer (5 to 20 μm) than most bacteria, and has a spirally twisted shape. The flagella are short in relation to the size of the cell. One reasonable counterargument to the view that flagellar rotation is "unbiological" is based on the fact that for many years bacteriologists accepted the idea that the special motion of *Spirillum* is generated by flagellar rotation (Weibull (1960, p. 166)). During motion, the flagella all rotate in the same sense about a longitudinal axis, each tuft being visible as a blurred cone. The body reacts by rotation in the opposite sense which, because of its spiral shape, propels it through the medium (Chwang, Wu and Winet (1972)).

Superficially, members of the order Spirochaetales resemble *Spirillum*, but their locomotion is quite different and does not really come within my subject because they are completely without flagella. The only analogous structure they possess is a fibril spirally wound (quite tightly) around the spirally shaped body. Problems of how it and other features of the organisms may act to make possible a helical propulsive motion with longitudinal moments in balance remain exceedingly challenging and probably farther from a solution than any that we have encountered in this brief tour of Fig. 1 (for an excellent modern analysis, see Chwang, Winet and Wu (1974)).

I shall now conclude that tour by mentioning the extraordinary symbiotic relationship between a trichomonad flagellate *Mixotricha paradoxa* (500 μm long) and a very large number of adherent spirochaetes (about 10 μm long) attached all over its surface by special "brackets" to give it the appearance of a ciliate. The highly complex symboisis that is involved (Cleveland and Grimstone (1964)) produced convergence on a mode of locomotion, with coordinated waving of the dense mass of attached spirochaetes, that is quite uncannily similar to the locomotion of ciliates with somatic ciliature.

2.4. Flagellar structures. Now I shall supplement what I have said about flagellar motions with some brief notes about the structures of the two fundamentally quite different kinds of flagella of which I have been speaking, beginning with the perhaps simpler bacterial flagellum. In electron micrographs of bacterial flagella (Fig. 2) it is always possible to distinguish two quite different parts: the proximal highly curved region called the "hook" (about 4 diameters

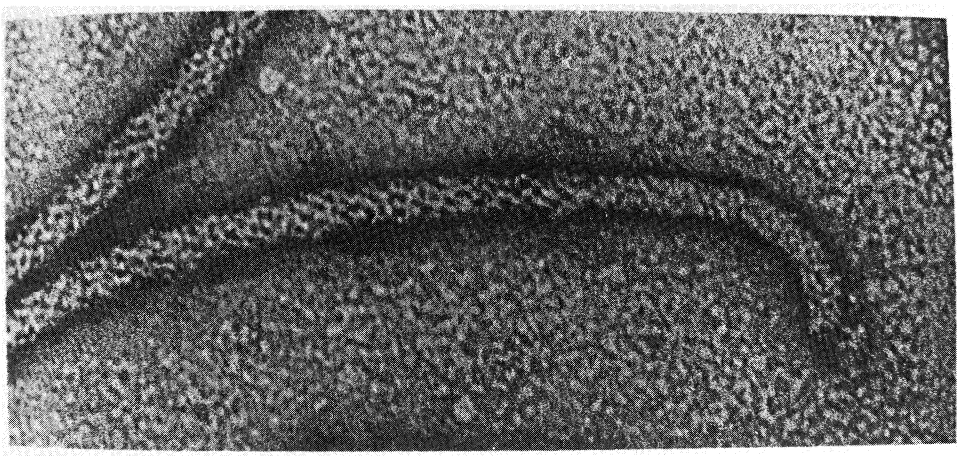

FIG. 2. *An intact bacterial flagellum and hook:* ×500,000 (*Smith and Koffler* (1971))

long) and the remaining region with relatively much lower curvature, called the flagellar filament proper. There is clear evidence of a *relatively looser* connection between hook and filament—that is, a connection whose strength is less than that of the components separately—since mechanical or chemical methods of detaching flagella from bacteria frequently also detach the hooks from the filaments (Fig. 3).

FIG. 3. *Detached flagella and hooks* (*Smith and Koffler* (1971))

A differential solubility of hooks and filaments can be further used to isolate a preparation consisting of hooks alone (Fig. 4). Chemical analysis of isolated hooks, and of isolated filaments, has demonstrated definite chemical differences, although these are relatively minor differences between proteins of broadly similar primary structure (Smith and Koffler (1971, p. 237)).

The protein of which flagellar filaments are made is relatively well known (because it has been isolated for much longer and in large quantities) and is called flagellin. Each species of bacterium produces a different flagellin with slightly but not greatly different amino-acid composition (Smith and Koffler (1971, p. 240)). Molecular weights are in the range 30,000 to 50,000.

The most characteristic property of flagellin is its ability to assemble into flagella-like filaments (Fig. 5). Both these reconstituted filaments and natural flagellar filaments are in the form of helical tubes with empty central core (Smith

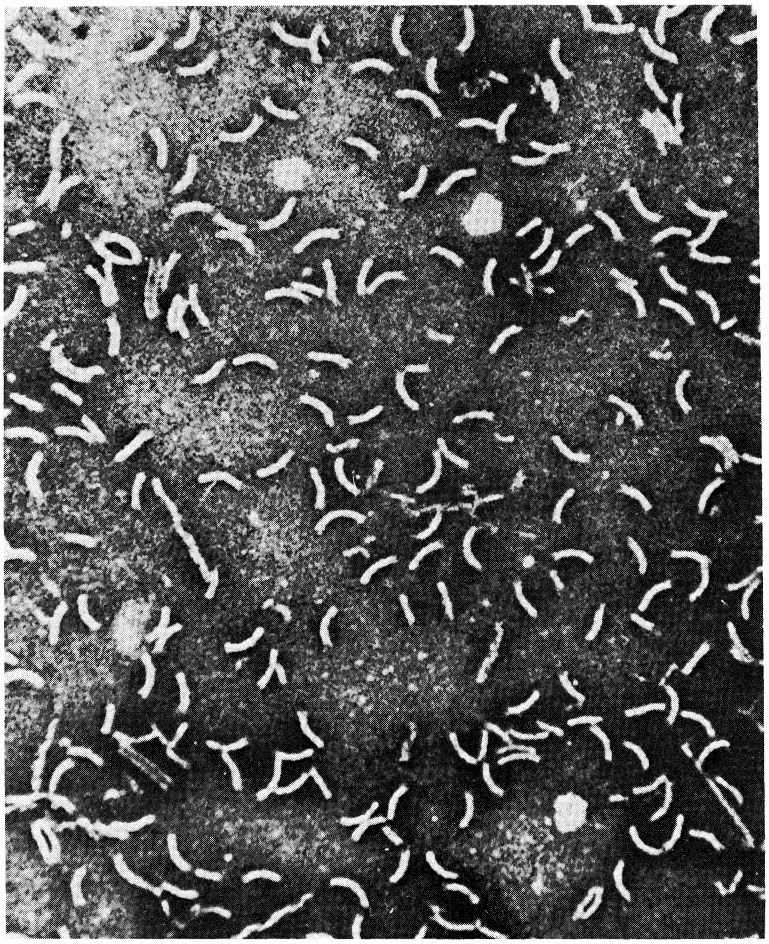

FIG. 4. *Preparation of hooks alone* (*Smith and Koffler* (1971))

and Koffler (1971, p. 282): see also Fig. 6). Such a tubular structure accords with various possible arrays of flagellin subunits that have been hypothesized.

Many different mutant forms of bacteria without normal motility have been produced. Certain mutants of *Salmonella* are unable to move their flagella, although those flagella themselves are immunologically indistinguishable from those of normal cells. This is at least consistent with the rotary hypothesis that the source of motion is not in the filament itself but in the rotation of a basal structure to which the hook attaches it.

Mutants were used by Silverman and Simon (1974) to obtain evidence very strongly in support of the rotary hypothesis. For some time it had been known that a peritrichous bacterium might become attached by *one* of its flagella to the glass of a microscope slide, and would then be seen to rotate for an extended period. This observation was again consistent with the view that the flagellum is attached to a basal structure which rotates relatively to the cell, so that fixing the flagellum

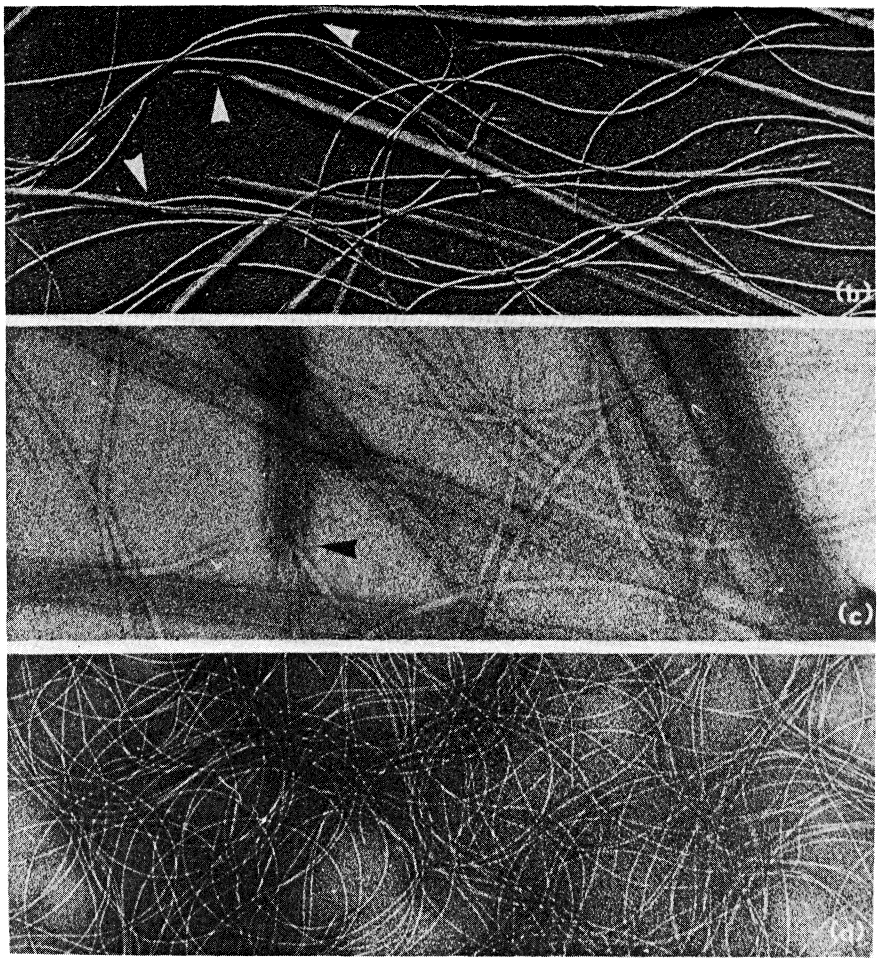

FIG. 5. *Flagella-like filaments reconstituted from flagellin in solution* (*Smith and Koffler* (1971))

causes the cell to rotate in the opposite direction. That argument is not at all conclusive, however, because the cell's rotation could possibly be generated by the motile activity of the other flagella. To exclude that possibility, Silverman and Simon (1974) carried out a variety of experiments on *Escherichia coli*:

(i) experiments with normal cells where a protein-deficient diet has been used to limit flagellin synthesis, to such an extent that the cell possesses only one flagellum of significant length; nevertheless, when that flagellum is attached to a slide the cell body shows the usual speed of rotation;

(ii) experiments with mutant cells whose flagella are straight and have been found unable to produce *any* locomotion; the cell attached by one of those straight flagella nevertheless shows the usual speed of rotation;

(iii) experiments with a mutant which synthesizes no flagellar filaments at all but only extended "hook" regions called "polyhooks" which again are unable to produce locomotion; nevertheless the polyhook originates from the basal region

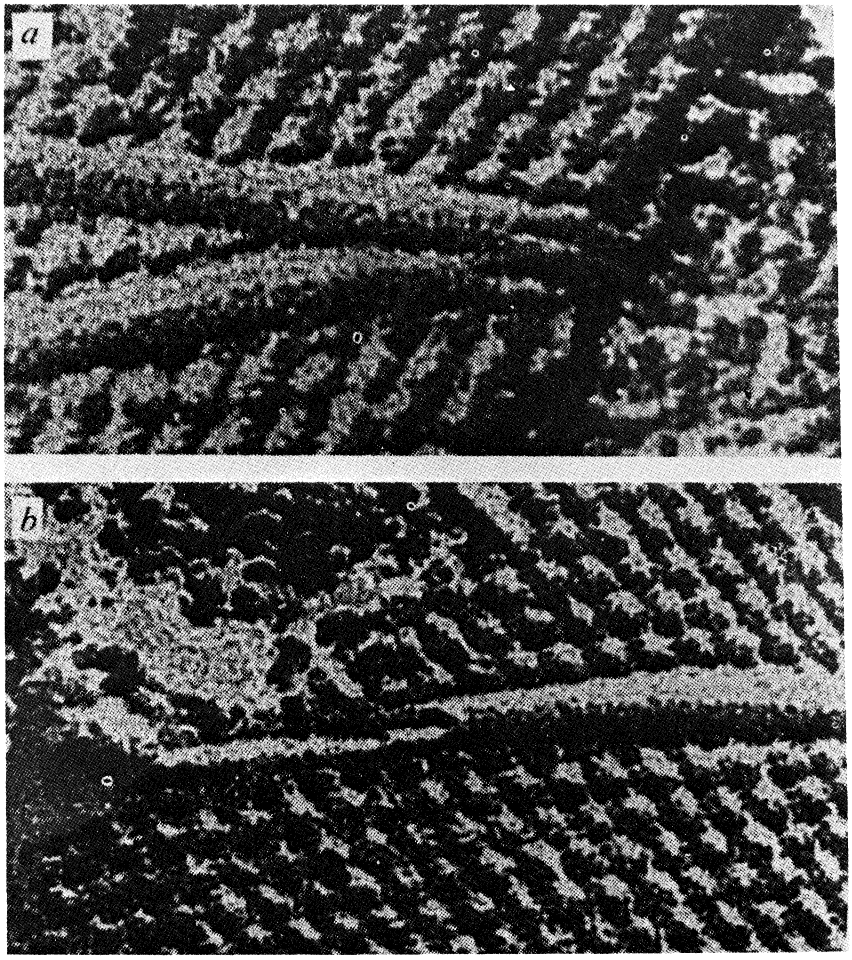

FIG. 6. *An empty core is visible (Slaytr and Glauert (1973)) in electron micrographs of cross-fractured bacterial flagella: a,* ×200,000; *b,* ×140,000

just like a normal hook and appears to be rotated relative to the cell body in the normal way because the cell body is again seen to rotate in the opposite direction.

Specifically, the cell rotates for tens of minutes at around 1000 revolutions a minute! Almost all the time it is rotating anticlockwise as observed on the microscope slide (in agreement with the idea of a rotary "motor" tending to turn the flagellum clockwise relative to the cell body), but there are brief periods of rotation in the opposite sense. This is consistent with the view that the "twiddles" are brief periods of anticlockwise rotation of one or more flagella.

Strong confirmation of this view is provided by the further work of Larsen, Reader, Kort, Tso and Alder (1974). Using the "polyhook" mutant, they showed that the normal tendency to anticlockwise rotation was reversed by additions of "repellent" solvents, in agreement *both* with the observed tendency of such solvents to generate frequent twiddles *and* with the proposed association of twiddles with reversal of rotation.

Much work remains to be done before a clear picture of the postulated rotary motor can emerge. Fig. 7 is a diagrammatic sketch pieced together by Berg (1974) from the fragmentary evidence so far available.

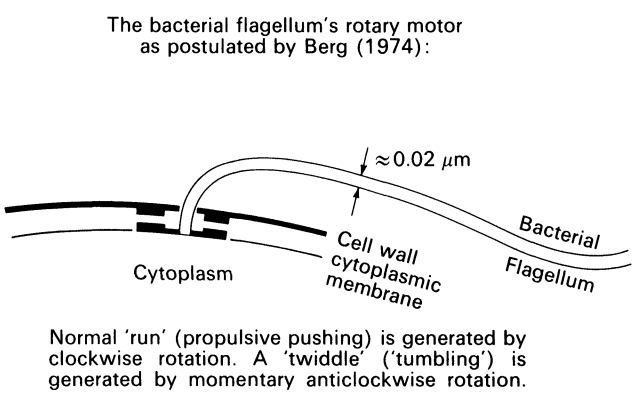

FIG. 7. *The bacterial flagellum's rotary motor as postulated by Berg* (1974)

It will also be of great importance to elucidate the special role of the hook. In a peritrichous bacterium the expeditious formation of a new flagellar bundle after each twiddle might be accelerated if the hook could flexibly *transmit the rotation* generated by the "motor" *round the 90° bend.* (This would be analogous to the apparent capacity of the proximal portion of the flagellum of *Euglena* for transmission of a rotation around a 180° bend.)

Hydrodynamic studies may play a significant role in answering questions like this and also questions about the characteristics of the motor and the influence of flagellar deformability. Such studies can begin from existing data on bacterial locomotion in fluids of different viscosity (see, for example, Schneider and Doetsch (1974) and the discussions by Berg and Anderson (1973) and Berg (1974)). Different observers agree with swimming speed in many different species *increases* somewhat as the viscosity increases above that of water, although decreasing at viscosities beyond about 5 times that of water. However, it remains hard to disentangle the possible influences contributing to these effects: for example, (i) the characteristics of the motor, (ii) the effects of flagellar deformability tending to compress (shorten) the helix at high thrusts, (iii) opposing hydrodynamic effects tending to increase cohesion of the bundle when viscous forces are large, and (iv) the effects of the helix angle (see § 3) on hydrodynamic efficiency.

By comparison with the extremely recent experiments described above that gave such strong support to the rotary hypothesis for bacterial flagella, it was earlier by some few years that the critical experiments throwing light on the mode of action of eukaryotic flagella took place. Work refining the description of the axoneme (9 + 2 structure) proceeded in parallel with work identifying its fundamental method of functioning.

We can now say (Ringo (1967), Warner (1970), Warner and Satir (1973)) that the axoneme consists of 9 doublet-tubules equally spaced in a circle

surrounding 2 singlet-tubules (Fig. 8). The doublet-tubule is made up of a complete tubule of circular cross section, called an A tubule, clutched by another so-called B tubule whose cross section is an incomplete circle. On the *other* side of the A tubule are the "limbs" that it uses (as is now supposed) to "walk" along the adjacent doublet-tubule.

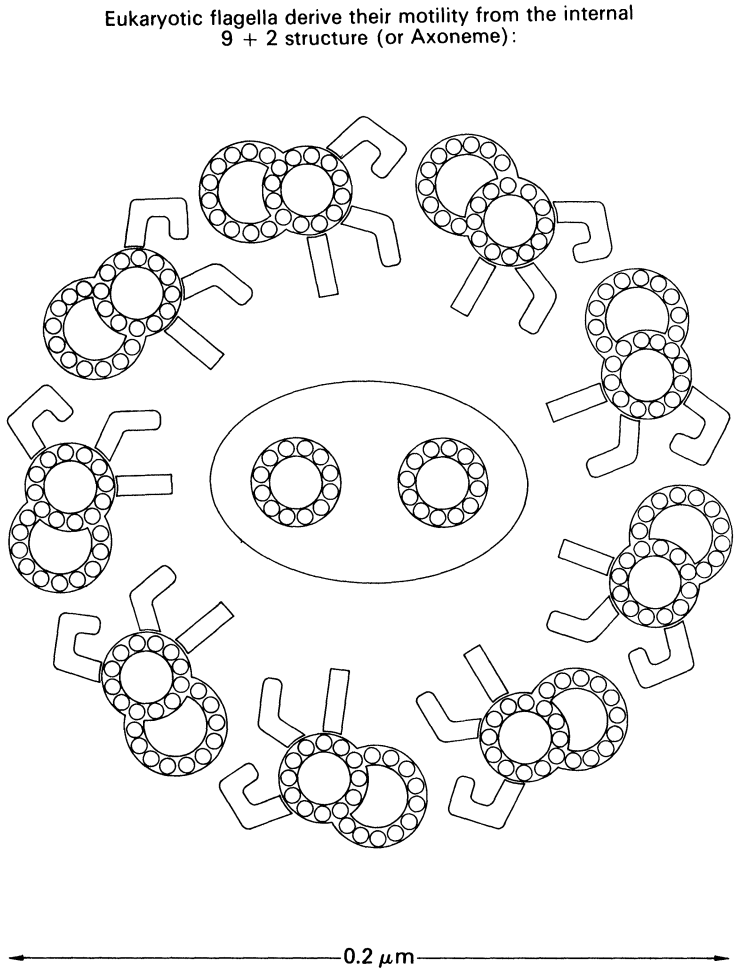

FIG. 8. *Axoneme structure, after Warner and Satir* (1973)

Some details of the finer structure of the A and B tubules are also given in Fig. 8. The protein of which they are composed, often called tubulin, is closely similar to the well-known protein actin that occurs in muscle fibers; its molecular weight is of order 50,000. The "limbs" are individual molecules of another protein called

dynein (Gibbons (1965)) which plays a role similar to the muscle-fiber protein myosin, and like it has a high molecular weight (of order 500,000) although its shape is quite different. "Walking" is believed to involve the breaking of existing chemical bonds between dynein limbs on an A tubule and molecules of tubulin on the B tubule of an adjacent doublet, followed by the formation of new bonds with molecules farther along the same B tubule. This (like the similar process with actin-myosin bonds in muscle) generates active shearing between adjacent doublet-tubules.

Another similarity to muscular activity is that this "walking" is *powered* by the dephosphorylation of ATP (adenosine triphosphate). The mitochondria in a flagellate cell generate the ATP which diffuses down the flagellum to activate the making and breaking of dynein-tubulin bonds.

Many of the fundamental experiments on the details of this activation process have been carried out on spermatozoa of higher animals. Nevertheless, the 9 + 2 structure of the axoneme is so closely similar throughout the vast majority of flagellate cells that it is reasonable to presuppose a common basic mode of action of axonenes with that stucture.

Summers and Gibbons (1971) worked with "naked" axonemes, obtained from sea urchin spermatozoa when the flagellar membranes that normally surround the axonemes are removed by "digestion" with a suitable biochemical agent. Naked axonemes, *unlike* normal flagella (consisting of an axoneme surrounded by a flagellar membrane), are directly sensitive to ATP in solution in the surrounding medium. Summers and Gibbons showed that this response to ATP always takes the form of an active sliding of doublet-tubules over neighboring doublet-tubules. Summers (1974) obtained identical results on bull sperm.

These findings strongly confirmed the conclusion of Satir (1968) to the effect that a flagellum bends by means of such active sliding *without any extensions or contractions of tubules.* Such a conclusion strongly contrasts with the classical behavior of an elastic rod, whose plane cross sections remain plane in the bent condition, leading to extension on the outside of the bend and contraction on the inside. Active sliding means that plane cross sections need not remain plane, so that bending becomes fully compatible with the inextensibility of each separate tubule.

Satir recognized that, with inextensible tubules of fixed total length, a flagellum or cilium with just one bend in it must have the *distal end* of a tubule on the inside of the bend protruding *beyond* the distal end of a tubule on the outside of the bend. His experiments on a cilium from the gill of a bivalve mollusc confirmed this, showing in fact that the extra amount by which the inner tubule protruded was exactly what would be predicted by this geometrical consideration if the tubules were supposed inextensible (Fig. 9). Then the work with "naked" axonemes confirmed the hypothesis of sliding of inextensible tubules by direct observation at all points along the tubule.

In the 9+2 structure, the role of the two singlet-tubules in the center has not yet been defined with conclusive precision (but see Warner and Satir (1974) for a detailed analysis of their recent data relevant to this matter). Speculatively, it is thought to be concerned with the control of the active-shear process. Those central tubules could be sensitive either to flagellar curvature, or to an integrated

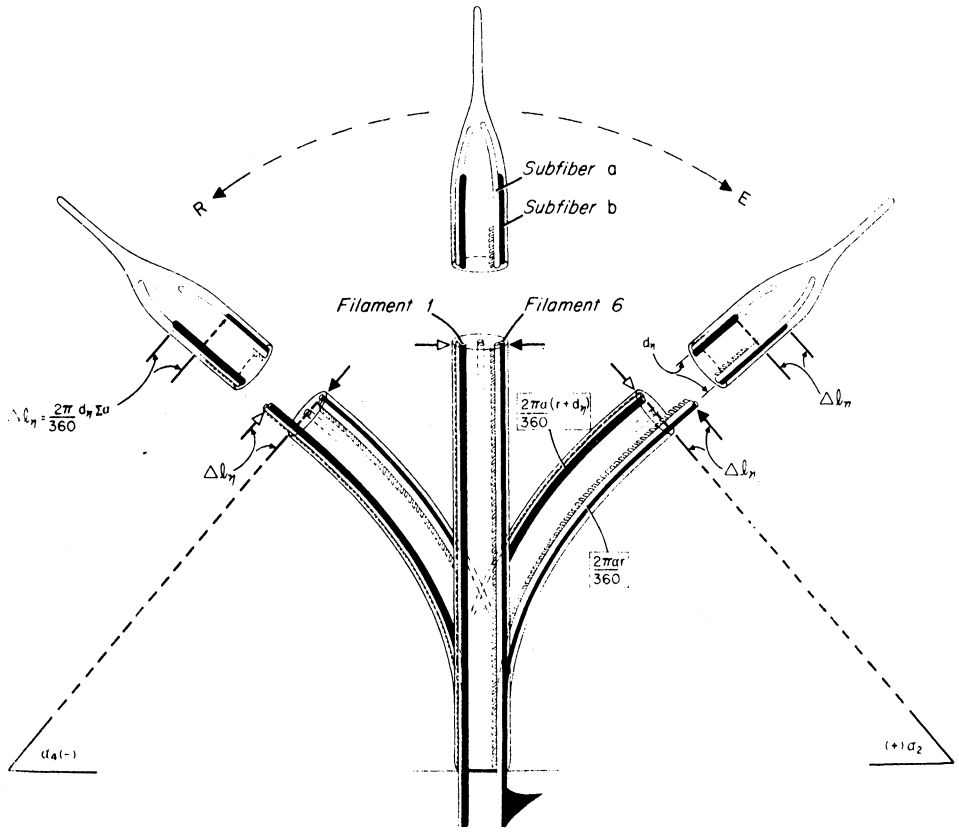

FIG. 9. *Model of flagellar bending, supported by the experimental work of Satir* (1968)

measure of changing curvature such as the sliding of doublet-tubules past them, or both. Various models for the propagation of both planar and helical waves down a flagellum have been discussed (see, for example, Brokaw (1972a), (1972b)). These different models make different assumptions regarding the active bending moments, or active shearing forces, generated by the "walking" of doublet-tubules as a response, either immediate or delayed, to variables such as could be sensed by the singlet-tubules.

The merits of those different models can, it is hoped, be evaluated by combining them with knowledge on flagellar hydrodynamics and comparing the resulting theoretical conclusions with observations in fluids of different viscosities. Extensive work on these lines has been attempted without, as yet, any conclusive results being reached. Nevertheless, the hope of ultimately reaching more precise conclusions in future studies of this kind remains a major incentive to those refinements of flagellar hydrodynamics which we attempt in § 3.

3. Application of mathematics to flagellar hydrodynamics.

3.1. Fundamentals of flagellar hydrodynamics. The motion of *fluid* around a microorganism follows the same rule as does the microorganism's own motion:

the forces on any particle of fluid are in equilibrium. The pressure force on such a particle is $-\text{grad } p$ per unit volume (acting down the pressure gradient), and the viscous force per unit volume is $\mu\nabla^2\mathbf{u}$ (representing a diffusive transfer of momentum brought about by the fluid's viscosity μ). The momentum equation

$$-\text{grad } p + \mu\nabla^2\mathbf{u} = 0 \tag{1}$$

equates the vector sum of these two forces to zero because, on the scale of a microorganism, fluid inertia is negligible. The velocity field $\mathbf{u}$ also satisfies the equation of continuity,

$$\text{div } \mathbf{u} = 0, \tag{2}$$

appropriate to an incompressible fluid.

Any *potential flow* $\mathbf{u} = \text{grad } \varphi$ (where $\nabla^2\varphi = 0$) satisfies these equations, with the pressure simply constant (because the viscous force vanishes). However, the set of potential flows is far too restricted to include any that satisfy the no-slip condition at a solid boundary, such as the surface of a microorganism. The velocity of the fluid at such a surface must equal the velocity of the solid surface itself; yet a potential flow is uniquely determined by requiring just the velocity components *normal* to the surface to match, which leaves a mismatch between the tangential velocity components.

For example, a dipole (or "source doublet") of vector strength $\mathbf{G}$ (directed *from* the negative *towards* the positive source) has

$$\varphi = \text{div}\left(\frac{\mathbf{G}}{4\pi r}\right), \qquad \mathbf{u} = \text{grad}\left[\text{div}\left(\frac{\mathbf{G}}{4\pi r}\right)\right], \tag{3}$$

if r is distance from the dipole. This velocity field $\mathbf{u}$ falls off rapidly as r increases, according to an inverse-cube law. On a particular spherical surface $r = a$, the *normal* components of $\mathbf{u}$ and of a constant vector $\mathbf{U}$ are equal if

$$\mathbf{G} = 2\pi a^3\mathbf{U}; \tag{4}$$

however, the dipole velocity field (3) would be compatible with a translational motion of the sphere $r = a$ at velocity $\mathbf{U}$ *only if slip* (*tangential* movement of fluid relative to the surface) were possible.

We widen the set of solutions of the Stokes equations (1) and (2) by including cases with nonuniform pressure p, which itself, however, must satisfy $\nabla^2 p = 0$ (divergence of (1)). A fundamental solution of great importance is the *stokeslet*, representing the effect of a concentrated external force $\mathbf{F}$ acting at a single point of the fluid; that is, of a delta function distribution of force per unit volume which modifies the force-balance equation (1) to become

$$\mathbf{F}\delta(\mathbf{r}) - \text{grad } p + \mu\nabla^2\mathbf{u} = 0. \tag{5}$$

Here $\mathbf{r}$ stands for vector displacement from the point of application of the force. Taking the divergence of (5) gives

$$\nabla^2 p = \text{div}\,[\mathbf{F}\delta(\mathbf{r})], \tag{6}$$

whose solution for p is the potential

$$p = \operatorname{div}\left(-\frac{\mathbf{F}}{4\pi r}\right) \tag{7}$$

of a dipole. The strength of the dipole is $(-\mathbf{F})$ with the convention adopted above (*unlike* that used in Lighthill (1975) with the vector strength pointing from the positive towards the negative source).

The associated velocity field $\mathbf{u}$ can be written in many different ways. One of those is as

$$\mathbf{u} = \frac{\mathbf{F}}{6\pi\mu r} + \frac{1}{4} r^2 \operatorname{grad}\left[\operatorname{div}\left(\frac{\mathbf{F}}{6\pi\mu r}\right)\right]. \tag{8}$$

Both terms in the stokeslet velocity distribution (8) share the famous *inverse-first-power* dependence on r (the distance from the point of application of the force). The first term, with the same r^{-1}-dependence in every direction, represents the *spherical mean* of $\mathbf{u}$ (average value over a sphere of radius r); the second term modifies this with second order surface harmonics (e.g., by a factor $1+\frac{1}{2}P_2(\cos\theta)$ for the component parallel to $\mathbf{F}$). However, it is the second term in (8) which entirely generates the viscous force to balance the gradient of the pressure distribution (7); the first term generates no viscous force but must be incorporated in (8) if the equation of continuity (2) is to be satisfied (Lighthill (1975)).

On a given spherical surface $r = a$, the second term in (8) can be completely cancelled by adding on a dipole velocity field (3) of strength

$$\mathbf{G} = -\frac{a^2\mathbf{F}}{6\mu}. \tag{9}$$

The fluid velocity on $r = a$ then takes a constant value

$$\mathbf{U} = \frac{\mathbf{F}}{6\pi\mu a}. \tag{10}$$

The combined stokeslet $\mathbf{F}$ and dipole $\mathbf{G}$ can therefore represent a fluid motion for $r \geqq a$ which matches perfectly with the translational motion at velocity $\mathbf{U}$ of a solid spherical boundary $r = a$. The sphere acts on the fluid with a net force satisfying the Stokes relationship (10). Amusingly enough, the required dipole strength (9) can be written as $-\pi a^3\mathbf{U}$, *opposite in sign* to the value (4) that generates the *irrotational* flow field with just the normal components of velocity matched.

This Stokes formula (10) for the force $\mathbf{F}$ required to move a sphere at velocity $\mathbf{U}$ can be written

$$\mathbf{F} = 11.66\mu\mathbf{U}V^{1/3} \tag{11}$$

in terms of the sphere's volume $V = \frac{4}{3}\pi a^3$. The work of Pironneau (1973) and Bourot (1974) shows that the coefficient 11.66 in (11) is not far above the *minimum possible* value for resistance to motion of a body of volume V; this minimum coefficient of 11.13 is attained for axial motion of the body of revolution shown in Fig. 10. Such drag formulas for shapes similar to cell bodies of microorganisms are of importance in flagellar hydrodynamics because they

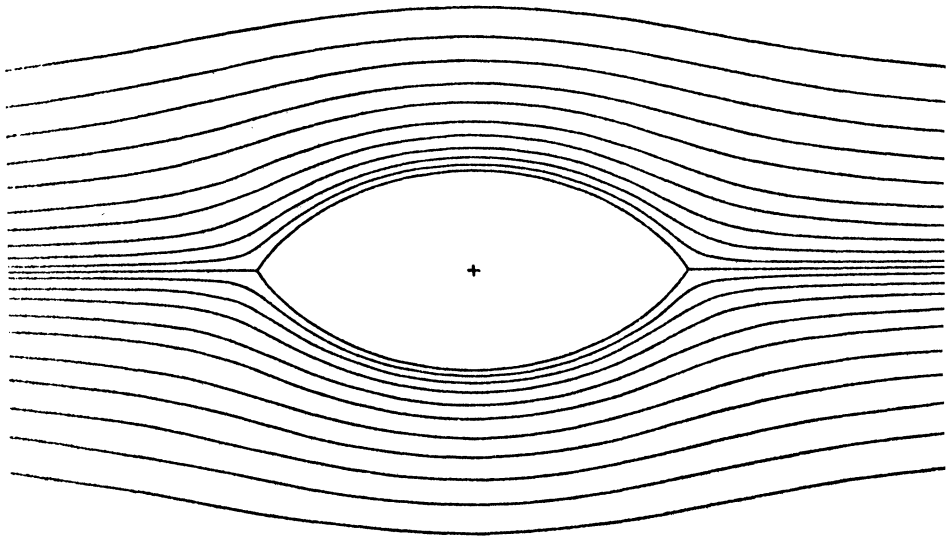

FIG. 10. *Shape having the least resistance, among bodies of revolution of given volume moving axisymmetrically with given velocity (Bourot (1974)); some streamlines of the fluid flow relative to the body are also shown*

suggest how much thrust an attached flagellum must provide to propel the organism at a given velocity.

It is worth emphasizing that the classical paradox concerning the inverse-first-power "stokeslet" velocity distribution (8), namely the fact that in unbounded fluid it has infinite energy, completely disappears in these applications to swimming microorganisms. Because the *total force* on the organism is zero (§ 1), its *total reaction* on the water must be zero. Thus, the flow field is a combination of (i) stokeslet fields associated with flagellar thrust and (ii) stokeslet fields associated with equal and opposite cell body drag. Because the vector sum of all the stokeslet strengths in zero, the inverse-first-power terms in the combined far fields must cancel. Accordingly, the kinetic energy of the fluid takes a sensible finite value (without any modified theory based on the "Oseen equation" having to be introduced).

The flow field due to the thrusting action of a flagellum may be described (see below) by use of a distribution of stokeslets along its centerline, representing the instantaneous distribution of forces with which different parts of the flagellum act on the fluid. Dipoles may be combined with the stokeslets (rather as in the spherical case) so that the velocity field closely satisfies the boundary condition for a particular flagellar motion, *related to* the assumed force distribution. Finally, if this relationship can be inverted, then the force distribution may be known for a given flagellar motion, to a far better approximation than if Gray–Hancock resistance coefficients were used.

With such a program in mind, I first rewrite the stokeslet velocity distribution (8) with the differentiations of r^{-1} carried out explicitly as

$$\mathbf{u} = \frac{r^2\mathbf{F} + (\mathbf{F}\cdot\mathbf{r})\mathbf{r}}{8\pi\mu r^3}: \tag{12}$$

a vector field which is the sum of a *parallel* field and a *radial* field. Then I state the relationship of flagellar motion to flagellar force distribution in a style appropriate to a mathematical commemorative lecture as follows.

THEOREM 1. *If* $\mathbf{f}(s)$ *is the force per unit length with which a flagellum of small radius* a *acts on a fluid, where the variable* s *signifies length measured along the centerline of the flagellum from some given cross section, then the resulting fluid motion can be represented by a distribution of stokeslets along the centerline, of strength* $\mathbf{f}(s)$ *per unit length, accompanied by dipoles of strength*

$$-\frac{a^2\mathbf{f}_n(s)}{4\mu} \tag{13}$$

per unit length; here $\mathbf{f}_n(s)$ *is the vector normal to the centerline obtained by resolving* $\mathbf{f}(s)$ *onto the plane normal to the centerline. This fluid velocity field* $\mathbf{u}$ *closely matches flagellar motions* $\mathbf{w}$ *such that the whole cross section where* $s = s_0$ *moves with velocity*

$$\mathbf{w}(s_0) = \frac{\mathbf{f}_n(s_0)}{4\pi\mu} + \int_{r_0>\delta} \frac{r_0^2\mathbf{f}(s) + [\mathbf{f}(s)\cdot\mathbf{r}_0]\mathbf{r}_0}{8\pi\mu r_0^3}\, ds; \tag{14}$$

here $\delta = \frac{1}{2}a\sqrt{e} = 0.82a$ *and* $\mathbf{r}_0$ *is the position vector of the point* s_0 *on the centerline relative to the point* s.

Historical notes. The general idea of Theorem 1 and of its proof was given in special cases by Hancock (1953) before he joined Sir James Gray to produce an approximate result in terms of resistance coefficients (Gray and Hancock (1955)). Results similar to Theorem 1 were given in very general cases by Batchelor (1970) and Cox (1970), who used a series expansion in integer powers of a parameter $\varepsilon = [\ln(2l/a)]^{-1}$, where l is a flagellar length scale. Retention of one or two terms in such an expansion involves errors whose magnitude depends on the size of the *logarithm* of $2l/a$ (which, for example, may only be 4.6 for $2l/a = 100$). The word "closely" is used in Theorem 1 to indicate that, by contrast, the error in (14) tends to zero *linearly* (rather than logarithmically) as $(a/l) \to 0$.

Interpretative notes. Theorem 1 is stated in terms of a single flagellum but can be regarded as applying equally to more than one flagellum with different ranges of s used for different flagella. Equation (14) gives only the flagellar velocity associated with the *flagellar* force distribution; the total flagellar velocity includes a contribution from the flow field generated by the movement of the cell body. For movements close to a microscope slide, Theorem 1 needs to be modified by including with each stokeslet the effects of its image system in that plane solid boundary (Blake (1971)). Finally, I reemphasize that practical use of (14) must involve some form of *inversion* of the relationship to derive the force distribution $\mathbf{f}(s)$ in terms of the flagellar velocity distribution $\mathbf{w}(s)$. Equation (14) makes this computationally feasible because it relates those two distributions as functions of just one independent variable s, representing position on the centerline, with all variations at right angles to the centerline completely eliminated.

Sketch of a proof of Theorem 1. The proof that the whole surface of the cross section at s_0 moves with the velocity (14) is facilitated by a special choice of axes with origin O at the center of that cross section and x-axis tangential to the

centerline. The main point that needs to be established is that contributions of stokeslets close to the origin O (with $r_0 < q$, where q is a *large* multiple of the radius a, but a *small* fraction of a flagellar wavelength) produce, together with their associated dipoles (13), a surface velocity given by (14) with the integral limited to $r_0 < q$. In fact (12) shows that the other stokeslets, at distances $r_0 > q$, generate *at the cross section center* O a velocity given by the integral (14) limited to $r_0 > q$; but they are far enough away from O for (i) the velocity field they generate to vary negligibly over the cross section of radius a centered on O, and for (ii) the inverse-cube velocity fields due to their accompanying dipole distributions (13) to be negligible at that cross section.

As regards the contribution from singularities within $r_0 < q$, we may verify first that they take the form (14) in the simplest case when in that region the flagellum is effectively cylindrical, and $\mathbf{F}(s)$ is effectively a constant vector (f_x, f_y, f_z). Then (12) shows that the velocity field generated by the *tangential* stokeslet distribution f_x (with which *no* dipole distribution (13) is associated) can be written

$$\int_{-q}^{q} \frac{f_x}{8\pi\mu}\left(\frac{1}{r}+\frac{(x-X)(x-X)}{r^3}, \frac{(x-X)y}{r^3}, \frac{(x-X)z}{r^3}\right) dX, \tag{15}$$

where

$$r=[(x-X)^2+y^2+z^2]^{1/2} \tag{16}$$

represents distance from a stokeslet at $(X, 0, 0)$. Now on the surface of the cross section $x=0$, $y^2+z^2=a^2$, we have $r=(X^2+a^2)^{1/2}$. The y- and z-components of (15) are then zero (each as the integral of an odd function of X), while its x-component can be evaluated, through an integration by parts in its second term, as

$$\frac{f_x}{8\pi\mu}\left(\int_{-q}^{q} \frac{dX}{r}-\left[\frac{X}{r}\right]_{-q}^{q}+\int_{-q}^{q} \frac{dX}{r}\right)=\frac{f_x}{8\pi\mu}\left[4\sinh^{-1}\left(\frac{q}{a}\right)-\frac{2q}{(q^2+a^2)^{1/2}}\right]. \tag{17}$$

With an error of order $(a/q)^2$, we can replace (17) by

$$\frac{f_x}{8\pi\mu}\left(4\ln\frac{2q}{a}-2\right)=\frac{f_x}{8\pi\mu}\left(4\ln\frac{q}{\delta}\right) \tag{18}$$

with $\delta=\frac{1}{2}a\sqrt{e}$. This is the same as

$$\int_{\delta<r_0<q} \frac{f_x}{8\pi\mu}\frac{2ds}{r_0}, \tag{19}$$

which is exactly the contribution to the x-component of (14) from the f_x-component of $\mathbf{f}(s)$ in $r_0 < q$.

Similarly, the velocity field generated by the stokeslet distribution f_y, with its accompanying dipole distribution $-a^2 f_y/4\mu$, is

$$\int_{-q}^{q} \frac{f_y}{8\pi\mu}\left[\left(\frac{(x-X)y, r^2+y^2, yz}{r^3}\right)+\frac{1}{2}a^2\left(\frac{-3(x-X)y, r^2-3y^2, -3yz}{r^5}\right)\right] dX, \tag{20}$$

which on the cross section $x=0$, $y^2+z^2=a^2$, is easily evaluated because, with $O(a/q)^2$ again neglected,

$$\int_{-q}^{q}\frac{dX}{r^3}=\frac{3}{2}a^2\int_{-q}^{q}\frac{dX}{r^5} \tag{21}$$

(both taking the value $2/a^2$), so that the terms in y^2 and yz that vary round the cross-sectional surface cancel out. Accordingly, (20) has y-component

$$\frac{f_y}{8\pi\mu}\left(2\ln\frac{2q}{a}+1\right)=\frac{f_y}{4\pi\mu}+\frac{f_y}{8\pi\mu}\left(2\ln\frac{q}{\delta}\right), \tag{22}$$

which is the contribution

$$\frac{f_y}{4\pi\mu}+\int_{\delta<r_0<q}\frac{f_y\,ds}{8\pi\mu r_0} \tag{23}$$

to the y-component of (14) from the f_y-component of $\mathbf{f}(s)$ in $r_0<q$. The proof for the z-component f_z proceeds exactly as for the y-component.

Although the above proof was limited to the very restrictive condition of uniform stokeslet distribution and zero centerline curvature in $r_0<q$, we can readily verify that departures from these conditions are unimportant if the radius a is much less than other lengths in the problem, the error varying *linearly* (rather than logarithmically) with that ratio of lengths. For example, if the centerline were the locus of $(X, \kappa X^2, 0)$, with the curvature κ in the plane $z=0$, then y must be replaced in (15) and (16) by $y-\kappa X^2$. This on the cross section $x=0$, $y^2+z^2=a^2$ makes

$$r=[X^2+(y-\kappa X^2)^2+z^2]^{1/2}, \tag{24}$$

which to a first approximation in κ is

$$r=[(1-\kappa y)^2X^2+a^2]^{1/2}, \tag{25}$$

exactly as if X were replaced by $(1-\kappa y)X$. This produces relative errors $O(\kappa a)$ in the constancy of the velocity distributions (19) and (23) all around the cross section; that is, errors varying linearly with the ratio of the flagellar radius a to the radius of curvature of its centerline.

Again, the effect of nonuniformity in stokeslet distribution may be tested by inserting a factor $(1+\xi x)$ within the integrals (15) or (20) to allow for the effect of a component of the stokeslet distribution varying at a relative rate ξ per unit length of centerline. The result is to change (15) by an amount

$$(0, \xi y, \xi z)\frac{f_x}{8\pi\mu}\left(-2\ln\frac{2q}{a}+2\right), \tag{26}$$

representing a relative error $O(\xi a)$ varying linearly with the ratio of a to the length scale ξ^{-1} of variation of stokeslet strength. The same order of magnitude error is produced in (20).

By arguments along these general lines we can conclude that under flagellar conditions a close approximation to the velocity distribution (14) is produced all

over the cross section. This conclusion is applied to several problems of flagellar hydrodynamics in the sections that follow.

3.2. Spiral flagellar motions. It is natural to investigate in the first place those spiral flagellar configurations which were shown in §§ 2.2 and 2.3 to be so important for eukaryotic and bacterial flagella respectively. I begin with a clarification of the kinematics of the different motions that can occur, including spiral undulations and corkscrew rotations, confining myself in this section, however, to somewhat idealized spirals of constant radius and constant pitch.

A spiral undulation with constant radius b and constant pitch implies motions of the flagellar centreline which can be described by equations

$$y = b\cos[k(s-ct)], \qquad z = b\sin[k(s-ct)], \qquad x = \alpha s, \tag{27}$$

in terms of the distance s measured along the centerline; note that the motions involve no rotation of the flagellar surface *about* the centerline. In (27), the axis of the spiral is taken as the x-axis, and the condition that the flagellum is inextensible may be written

$$(\partial x/\partial s)^2 + (\partial y/\partial s)^2 + (\partial z/\partial s)^2 = 1, \tag{28}$$

or

$$\alpha^2 + b^2k^2 = 1. \tag{29}$$

Any structure capable of generating bends, like the axoneme of the eukaryotic flagellum, can generate such a spiral undulation by the simultaneous propagation of bends in the y- and z-directions.

It must be emphasized that the motions described by equations (27) include no translation (that is, swimming) or rotation. Any translation or rotation that they induce in the organism as a whole must be added on (see below) to give a description of the whole flagellar motion.

The undulation (27) has a wavelength Λ measured *along* the flagellar centerline equal to

$$\Lambda = 2\pi/k, \tag{30}$$

and a "pitch" (wavelength measured along the x-axis, which is the axis of the spiral) equal to

$$\lambda = \alpha\Lambda = 2\pi\alpha/k. \tag{31}$$

The wave travels *along the curved centerline* at velocity c, corresponding to propagation in the x-direction at velocity

$$V = \alpha c; \tag{32}$$

this V, of course, is the speed of the wave along the axis of the spiral relative to a fixed position on the flagellum such as its base or tip. Note also that equation (27) represents a right-handed or left-handed spiral according as the *system of axes* (x, y, z) is right-handed or left-handed.

Because there is always instantaneous equilibrium between the forces acting on a microorganism, or between those forces (1) that act on a nearby particle of

fluid, flagellar hydrodynamics can always be completely analyzed at a single instant of time, say, $t = 0$. At that instant, a point on the centerline (27) has *position* (x, y, z) equal to

$$(\alpha s, b \cos ks, b \sin ks) \tag{33}$$

and velocity $(\dot{x}, \dot{y}, \dot{z})$ equal to

$$\mathbf{w} = (0, bkc \sin ks, -bkc \cos ks). \tag{34}$$

The unit vector tangential to the centerline is

$$(\alpha, -bk \sin ks, bk \cos ks), \tag{35}$$

obtained by differentiating (33) with respect to s; equation (29) confirms that it has unit magnitude. Note that, as is true of any wave motion of constant amplitude, the motion of the centerline *relative* to the velocity $(V, 0, 0)$ of wave propagation is a purely *tangential* motion

$$\mathbf{w} - (V, 0, 0) = -c(\alpha, -bk \sin ks, bk \cos ks) \tag{36}$$

of *constant* speed c; in other words, the frame of reference travelling at the wave velocity is one in which the flagellum "appears stationary" because its motions are purely tangential.

We shall see that the spiral undulation (27) by itself (that is, in the absence of an additional swimming velocity of translation) fails to satisfy the conditions of instantaneous equilibrium because it generates a net thrust in the *negative* x-direction. Conversely, if a translational velocity $(-V, 0, 0)$ were superimposed on its motion, the flagellum would move purely tangentially (with negative x-component); a flagellar *drag* (force in the positive x-direction) would result, supplementing the drag on the cell body when moving at velocity $(-V, 0, 0)$ to produce a positive total drag on the organism. Evidently, at some intermediate velocity of swimming

$$(-U, 0, 0) \tag{37}$$

with $0 < U < V$, the necessary condition of zero net force on the organism can be met.

If the drag on the cell body were negligible, the organism would move at the *zero-thrust swimming speed* U_0, such that the spiral experiences zero net force when its centerline velocity is a linear combination of the fields (34) and (37). At this swimming speed, the drag opposing the spiral's tangential motions is just balanced by the thrust created by its normal motions. Often, any extra drag of the cell body may only slightly disturb this balance; in such a case the organism's swimming speed is only a little less than the zero-thrust value U_0.

On the other hand, we have seen in § 2.2 that the cell body may play a more significant role in balancing the *axial couple* generated by the spiral undulation of a eukaryotic flagellum. To make this quantitative, we first note that the velocity (34) of the point (33) on the flagellar centerline can be written

$$\mathbf{w} = (-\omega, 0, 0) \times (x, y, z), \tag{38}$$

with

$$\omega = kc. \tag{39}$$

This emphasizes the point, made many times in § 2, that in spiral undulation the motion of the flagellar centerline is exactly equivalent to a corkscrew-like rigid rotation of the instantaneous spiral shape (with angular velocity ω about the negative x-axis). Indeed, a bacterial flagellum (or flagellar bundle) of spiral form, being given (according to the rotary hypothesis) such an angular velocity ω, would experience *exactly the same motion* (38) of its centerline. (The only difference is that any rigid corkscrew rotation, unlike the spiral undulation, makes the flagellar *surface* rotate about its centerline; a distinction used in § 2.4 to evaluate the rotary hypothesis).

It is not surprising, since the spiral undulation (34) is equivalent to a centerline *rotation* (38) at an angular velocity (39) about the negative x-axis, that we shall find hydrodynamic forces acting on the spiral which give not only a thrust but also an opposing *positive* couple about the x-axis. Calculation of this couple is an important aim because, as we saw in § 2.2, it may act in various ways to determine the rotation of the organism as a whole—and hence to determine in many cases an additional rotary motion

$$(\Omega, 0, 0) \times (x, y, z) \tag{40}$$

which must be combined with the spiral undulation (38) and the translation (37) to give a total centerline velocity

$$\mathbf{w} = (-U, \omega_E b \sin ks, -w_E b \cos ks), \tag{41}$$

with the angular velocity of effective corkscrew rotation changed from $\omega = kc$ as in (39) to

$$\omega_E = \omega - \Omega. \tag{42}$$

We recall three interesting ways in which this modified effective rotation ω_E may be determined. In cases with a cell body on the axis of the flagellar spiral, but *without* activity in any secondary flagellum, Ω represents the rotation about the x-axis of the organism as a whole, and is *positive*, taking a value between 0 and ω such that the positive couple resisting effective corkscrew rotation with net angular velocity (42) is exactly balanced by the negative couple resisting cell body rotation at angular velocity Ω. Balancing the couples in this case reduces the effective corkscrew rotation and hence the swimming speed.

By contrast, Ω may be negative in two other interesting cases. Action of the transverse flagellum in dinoflagellates may reverse the rotation of the cell body, by acting on it with a negative couple. Alternatively, for *Euglena* it was argued in § 2.2 that a positive angular velocity of the cell body may generate (on transmission round a flexible 180° bend) a negative angular velocity Ω in the flagellum. In both cases, the effective corkscrew action is increased, leading to increased swimming speed.

To sum up the kinematics of spiral flagellar motions of constant radius b and constant pitch, the total velocity $\mathbf{w}$ of a general point (33) on the centerline can be written in the form (41) as a combination of:

(i) a translational motion (37) with swimming speed U;

(ii) an effective corkscrew motion (38), where $\omega = kc$ for a eukaryotic flagellum, while ω for bacterial flagella or bundles on the rotary hypothesis represents their actual velocity of corkscrew rotation;

(iii) an additional angular velocity $(\Omega, 0, 0)$ in either case, determined by the condition of zero net couple on the organism.

This distribution of $\mathbf{w}$ is now applied, with Theorem 1, to determine the distribution of the force $\mathbf{f}(s)$ per unit length with which the flagellum acts on the fluid.

In this section the analysis is carried out without reference to any special "end effects" at the tip or base of the flagellum; this avoids consideration of any special geometrical or kinematic features of the tip or base motions. In parts of the spiral *not* close to the ends, it is reasonable to seek a form for $\mathbf{f}(s)$ that is *invariant under any transformation* which leaves unaltered the equation (33) of the spiral: in particular, a shift in the origin of s to (say) s_0, together with a translation of the coordinate axes through a distance αs_0 in the x-direction and a rotation of them through an angle ks_0 about it. Such an invariant form

$$\mathbf{f}(s) = (g, h \sin ks, -h \cos ks) \tag{43}$$

(where g and h are constants) will indeed be found to give satisfactory results.

In this section we determine the *zero-thrust swimming speed*; namely, the value U_0 for which the centerline velocity distribution (41) is compatible with a force distribution (43) *with zero resultant*: that is, with $g = 0$; more general cases are postponed to § 3.4. In this case, the force distribution (43) acting on the fluid at the location (33) is equivalent to a couple per unit length:

$$(x, y, z) \times (0, h \sin ks, -h, \cos ks) = (-bh, 0, 0). \tag{44}$$

The equal and opposite reaction of the fluid on the flagellum is a positive couple about the x-axis, of magnitude bh per unit length, which, as discussed above, would be involved in determining Ω. The rate of working against this opposing couple is

$$E = \omega_E bh \tag{45}$$

per unit length. The zero-thrust swimming speed U_0 may be only a slight overestimate of U in cases where the cell body drag is small compared with the opposing forces competing to determine the net thrust on the flagellum.

In this case $g = 0$, the force distribution (43) has (according to (35)) a tangential component

$$(0, h \sin ks, -h, \cos ks) \cdot (\alpha, -bk \sin ks, bk \cos ks) = -hbk. \tag{46}$$

The vector $f_n(s)$ normal to the centerline referred to in Theorem 1 can be obtained by subtracting from $\mathbf{f}(s)$ its tangential resultant to give

$$\begin{aligned} \mathbf{f}_n(s) &= \mathbf{f}(s) + hbk(\alpha, -bk \sin ks, bk \cos ks) \\ &= h\alpha(bk, \alpha \sin ks, -\alpha \cos ks). \end{aligned} \tag{47}$$

We can now write down the equation (14) stated in Theorem 1; we choose to write it down at $s_0 = 0$, provided that this flagellar cross section which is the origin of s has been chosen far from the ends of the flagellum. It follows from the invariance of the vector quantities concerned under the coordinate transformation described above that the equation if satisfied at $s_0 = 0$ must be satisfied for any other s_0 not influenced by end effects.

By (41) with $U = U_0$, (43) with $g = 0$ and (47), the equation (14) with $s_0 = 0$ becomes

$$(-U_0, 0, -\omega_E b) = \frac{h\alpha}{4\pi\mu}(bk, 0, -\alpha) + \int_{r_0>\delta} \frac{r_0^2(0, h\sin ks, -h\cos ks) + (bh\sin ks)\mathbf{r}_0}{8\pi\mu r_0^3}\, ds, \tag{48}$$

where the position vector $\mathbf{r}_0$ of the point $s = 0$ on the centerline relative to the point s given by (33) is

$$\mathbf{r}_0 = (-\alpha s, b(1-\cos ks), -b\sin ks), \tag{49}$$

with magnitude

$$r_0 = [\alpha^2 s^2 + 2b^2(1-\cos ks)]^{1/2}. \tag{50}$$

Note that the y-components of both sides of the vector equation (48) are identically zero: in particular, the y-component of the right-hand side is the integral of an odd function of s which converges for large $|s|$.

The x-component of (48) gives

$$4\pi\mu U_0 = -h\alpha bk + h\alpha bk \int_\varepsilon^\infty \frac{\theta\sin\theta\, d\theta}{[\alpha^2\theta^2 + 2(1-\alpha^2)(1-\cos\theta)]^{3/2}}, \tag{51}$$

where the substitution $ks = \theta$ has been made in the integral, and

$$\varepsilon = k\delta = \tfrac{1}{2}(ka)\sqrt{e} = 0.82ka = 5.2(a/\Lambda), \tag{52}$$

and the integral of an even function of θ has been written as twice the integral for positive θ. The integrand in (51) behaves like θ^{-1} as $\theta \to 0$ but converges absolutely for large θ, so that the integral can be written

$$-\ln\varepsilon + A_1(\alpha), \tag{53}$$

where the function $A_1(\alpha)$ is easy to compute and is plotted in Fig. 11.

A different integral, appearing in the z-component of (48), can similarly be written

$$\int_\varepsilon^\infty \frac{\sin^2\theta\, d\theta}{[\alpha^2\theta^2 + 2(1-\alpha^2)(1-\cos\theta)]^{3/2}} = -\ln\varepsilon + A_2(\alpha), \tag{54}$$

where the function $A_2(\alpha)$ is also plotted in Fig. 11. On the other hand, one more integral appearing in the z-component of (48) may through an integration by parts

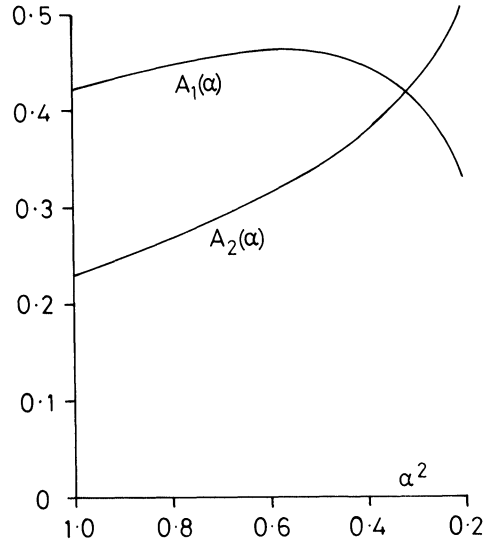

FIG. 11. *The functions* $A_1(\alpha)$ *and* $A_2(\alpha)$ *defined in* (53) *and* (54)

be expressed in terms of A_1 and A_2:

$$\int_\varepsilon^\infty \frac{\cos\theta\, d\theta}{[\alpha^2\theta^2+2(1-\alpha^2)(1-\cos\theta)]^{1/2}} = -\ln\varepsilon+\alpha^2A_1(\alpha)+(1-\alpha^2)A_2(\alpha)-1. \tag{55}$$

Accordingly, the x- and z-components of (48) become

$$\begin{aligned} 4\pi\mu U_0 &= h\alpha bk[-1-\ln\varepsilon+A_1(\alpha)], \\ 4\pi\mu\omega_E b &= h[-(1-\alpha^2)-(2-\alpha^2)\ln\varepsilon+\alpha^2A_1(\alpha)+2(1-\alpha^2)A_2(\alpha)]. \end{aligned} \tag{56}$$

The equations (56) are important in three ways. Their *ratio* gives the result

$$\frac{U_0}{V_E} = \frac{(1-\alpha^2)[-1-\ln\varepsilon+A_1(\alpha)]}{-(1-\alpha^2)-(2-\alpha^2)\ln\varepsilon+\alpha^2A_1(\alpha)+2(1-\alpha^2)A_2(\alpha)} \tag{57}$$

for the ratio of the zero-thrust swimming speed U_0 to the *apparent wave velocity* $V_E = \alpha\omega_E/k$ (apparent velocity of waves relative to the organism as modified by the corkscrew effect of the organism's own rotation). This is plotted in Fig. 12 as a function of $\alpha^2 = 1-b^2k^2$ for various values of Λ/a (where Λ is wavelength measured along the flagellar centerline), corresponding by (52) to values of $\varepsilon = 5.2a/\Lambda$.

Again, using (45), we can write the rate of working against the fluid per unit length of flagellum, E, in terms of the swimming speed U_0, as

$$\frac{E}{\mu U_0^2} = \frac{4\pi[-(1-\alpha^2)-(2-\alpha^2)\ln\varepsilon+\alpha^2A_1(\alpha)+2(1-\alpha^2)A_2(\alpha)]}{\alpha^2(1-\alpha^2)[-1-\ln\varepsilon+A_1(\alpha)]^2}. \tag{58}$$

This ratio is plotted in the lower part of Fig. 12. Although the minimum at around $\alpha^2 = 0.5$ had been suggested by theories using Gray–Hancock resistance coefficients (Holwill (1966, p. 773)), the absolute values of rate of working for given

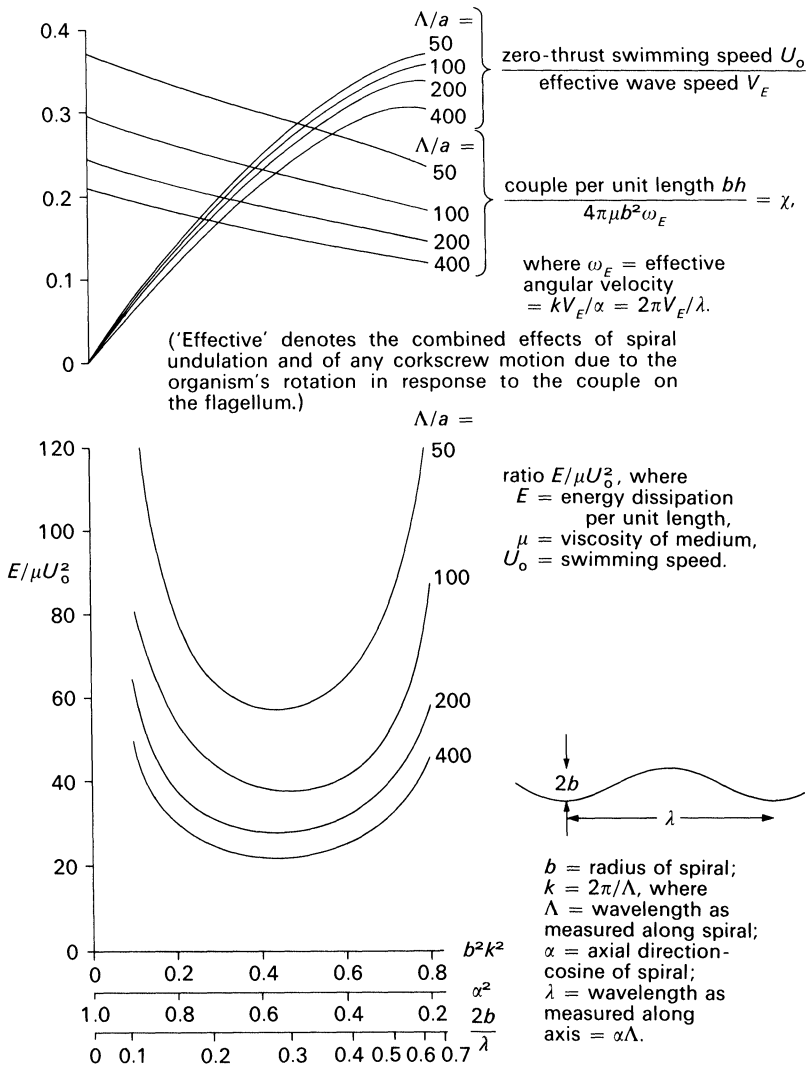

FIG. 12. *Zero-thrust swimming of spirals*

swimming speed obtained by use of those coefficients are much too low (see § 3.3 for a full discussion). At the bottom of Fig. 12, note also the alternative scale in terms of the aspect ratio $2b/\lambda$ of the spiral (ratio of diameter to pitch).

Lastly, equations (56) can be used to determine the couple bhL acting on a flagellum of total length L, of which a nondimensional form χ is plotted in Fig. 12. For some organisms, the angular velocity Ω of their rotation is determined by the condition that this couple is balanced by the couple $D\Omega$ resisting cell body rotation. Here D is the rotational damping coefficient of the cell body (couple resisting rotation at unit angular velocity). Then the balance equation

$$D\Omega = bhL = 4\pi\mu b^2\omega_E\chi L \tag{59}$$

can be used with (56) to determine the factor

$$\frac{V_E}{V}=\frac{\omega_E}{\omega}=\frac{\omega_E}{\omega_E+\Omega}=\left[1+\chi\frac{4\pi\mu b^2 L}{D}\right]^{-1} \tag{60}$$

by which the apparent wave velocity falls short of the real velocity of the wave as generated by the organism, or by which the effective angular velocity of rotation ω_E falls short of the value $\omega = kc$ obtained when the cell body does not rotate. Equation (58) confirms that the swimming speed U_0 is reduced by the same factor, which is easily obtained from the values of χ in Fig. 12 when the nondimensional form $D/(4\pi\mu b^2 L)$ of the rotational damping coefficient of the cell body is known.

Alternatively, on the hypothesis (§ 2.2) that the rotation of the cell body of *Euglena* induces an equal and opposite corkscrew rotation of the flagellum, equations (59) and (60) can still be used with the sign of D changed. In that case, the swimming speed U_0 is enhanced by a factor (60) which exceeds 1.

3.3. Suboptimal representations by local resistance coefficients. Although a particular flagellar motion like that of § 3.2 may be analyzed to good accuracy by means of Theorem 1, which also will be shown to yield admittedly more laborious analyses of further problems to similar accuracy in § 3.4, nevertheless for many crude studies it remains desirable (see § 1) to use a simple representation of flagellar dynamics by means of local resistance coefficients. In this section we investigate, through use of material derived from § 3.2, what values of the resistance coefficients may give best results in studies of typical flagellar motions. We seek, in other words, a *suboptimal representation* of flagellar dynamics by optimizing within the subset of representations of that dynamics by means of resistance coefficients.

The classical representation due to Gray and Hancock (1955) uses results which we found in passing during the proof of Theorem 1. The tangential velocity (18), generated all over the surface of a cross section by a tangential force per unit length f_x acting at all points within a distance q from it, suggests a local tangential resistance coefficient (force per unit length divided by velocity) equal to

$$K_T=\frac{2\pi\mu}{\ln(2q/a)-\frac{1}{2}}; \tag{61}$$

by contrast, the normal velocity (22), generated by a normal force per unit length f_y acting at all points within a distance q, suggests a normal resistance coefficient

$$K_N=\frac{4\pi\mu}{\ln(2q/a)+\frac{1}{2}}. \tag{62}$$

Unfortunately, these values are not uniquely determinate because they depend on the choice of q. However, the fact that this dependence is only logarithmic led Gray and Hancock to the view that a high degree of accuracy in the choice of q would not be important to a first approximation. In fact, they selected a value for q equal to one particular quantity with the dimensions of length characteristic of the problem: the flagellar wavelength λ.

There is one obvious criticism of this choice for q: it violates the assumption explicitly made in the proof of Theorem 1 that q is small compared with the

flagellar wavelength. This violation can be expected to be serious, especially because it grossly falsifies the assumption of uniform force per unit length applied by the flagellum within a distance q around a cross section. A preliminary study by Lighthill (1975) suggested that actually the resistance coefficients (61) and (62) may be much more reliable with

$$q/\lambda = 1/(2\pi e^{\gamma}) = 0.09, \tag{63}$$

where $\gamma = 0.577$ is Euler's constant. Evidently, this choice of q satisfies by a whole order of magnitude the requirement that it be small compared with λ; furthermore, some calculations for relatively small amplitude suggest that (63) is the preferred value in that case.

The differences between choosing $q = \lambda$ and $q = 0.09\lambda$ remain important even after logarithms have been taken as in (61) and (62). Various theoretical arguments which as just mentioned tend to support a choice near $q = 0.09\lambda$ were probably known to Gray and Hancock. On the other hand, they were aware of a practical difficulty associated with such a choice; namely, that the ratio of resistance coefficients,

$$r_K = K_T/K_N, \tag{64}$$

tends (Lighthill (1975)) to take a value (almost 0.7) *too large* to accord with observed ratios of swimming velocity to wave velocity. The fact that the choice $q = \lambda$, by reducing r_K much nearer to the limiting value 0.5, improves the agreement with those observed ratios seems to have weighed strongly with Gray and Hancock in making that choice.

Although preliminary attempts to resolve this conflict of arguments regarding the choice of q were made by Lighthill (1975), we shall find a more satisfactory resolution in this section. Essentially, (63) is the right choice for q (although for highest accuracy, λ should be replaced in it by the wavelength Λ measured along the curved flagellum), but a more careful calculation of K_T omits the $-\frac{1}{2}$ in (61). This confirms that the true resistance coefficients are much larger than Gray and Hancock supposed, but leaves their ratio (64) rather little changed.

To arrive at these conclusions, we find first what are the *effective resistance coefficients* in the zero-thrust spiral motions analyzed in § 2.2. The tangential velocity of the flagellum (scalar product of (35) and (41)) is

$$-U_0\alpha - \omega_E b^2 k. \tag{65}$$

The ratio of the tangential force per unit length (46) to this, by equations (56), is the tangential resistance coefficient

$$K_T = \frac{2\pi\mu}{-\ln \varepsilon - \frac{1}{2} + \alpha^2 A_1(\alpha) + (1-\alpha^2)A_2(\alpha)}. \tag{66}$$

On the other hand, the normal velocity of the flagellum (magnitude of the projection of (41) on to the plane normal to the flagellum) is

$$-U_0 bk + \omega_E b\alpha. \tag{67}$$

The ratio of the normal force per unit length (47), with magnitude $h\alpha$, to this is the

normal resistance coefficient

$$K_N = \frac{4\pi\mu}{-\ln \varepsilon + (2\alpha^2 - 1)A_1(\alpha) + 2(1-\alpha^2)A_2(\alpha)}. \tag{68}$$

The significance of these results can best be appreciated if we calculate the value of

$$\frac{4\pi\mu}{K_N} - \frac{2\pi\mu}{K_T}. \tag{69}$$

This is a quantity which greatly influences the degree of departure of r_K from 0.5. Furthermore, it is a quantity which on the Gray–Hancock models (61) and (62) must take the value 1 *whatever the value of q*. For zero-thrust spiral motions, however, the value of this quantity is

$$\tfrac{1}{2} + (1-\alpha^2)[A_2(\alpha) - A_1(\alpha)]. \tag{70}$$

Figure 13 (chain-dotted line) shows that this always remains substantially less than the Gray–Hancock value 1. For small-amplitude undulations (with $1-\alpha^2 = b^2k^2$ small), it is exactly $\frac{1}{2}$; furthermore, it remains close to $\frac{1}{2}$ for all values of the amplitude (falling a little below $\frac{1}{2}$ as the amplitude increases and then rising a little above it).

Note that for zero-thrust spiral motions, the resistance coefficients (66) and (68) by themselves can give as much information, and to the same good accuracy, as Theorem 1. In fact, analysis of the motion using those resistance coefficients would give accurate values of both the tangential and normal components of velocity (65) and (67), from which values of both U_0 and ω_E could be inferred agreeing exactly with the results (56) derived from Theorem 1 for a force distribution $(0, h \sin ks, -h \cos ks)$ exerted by the spiral (33). This makes it very interesting that expression (69) takes for these accurate resistance coefficients a value close to $\frac{1}{2}$ and not the value 1 which has hitherto been exclusively used.

In Fig. 13, the value of *q such that the accurate expression* (68) *for* K_N *coincides with the classical expression* (62) is also plotted (plain line), as a fraction of the wavelength $\Lambda = 2\pi/k$ (wavelength measured along the curved centerline of the flagellum). This value is

$$\frac{q}{\Lambda} = \frac{1}{2\pi} \exp\left[(2\alpha^2 - 1)A_1(\alpha) + 2(1-\alpha^2)A_2(\alpha) - 1\right], \tag{71}$$

which agrees in the small-amplitude limit $\alpha \to 1$ (when $A_1(\alpha) \to 1 - \gamma$ and $\Lambda \to \lambda$) with the value (63) proposed by Lighthill (1975) after calculations for normal distributions of stokeslets along flagella with small-amplitude undulations. Figure 13 shows, furthermore, that (q/Λ) remains close to this value 0.09 for all amplitudes. We conclude that normal resistance coefficients for zero-thrust spiral motions are the same as the values we obtain by calculating the normal velocity of a cross section resulting from a *uniform* distribution of normal force per unit length confined to within a distance 0.09Λ of that cross section, and ignoring the curvature of that same length of flagellum.

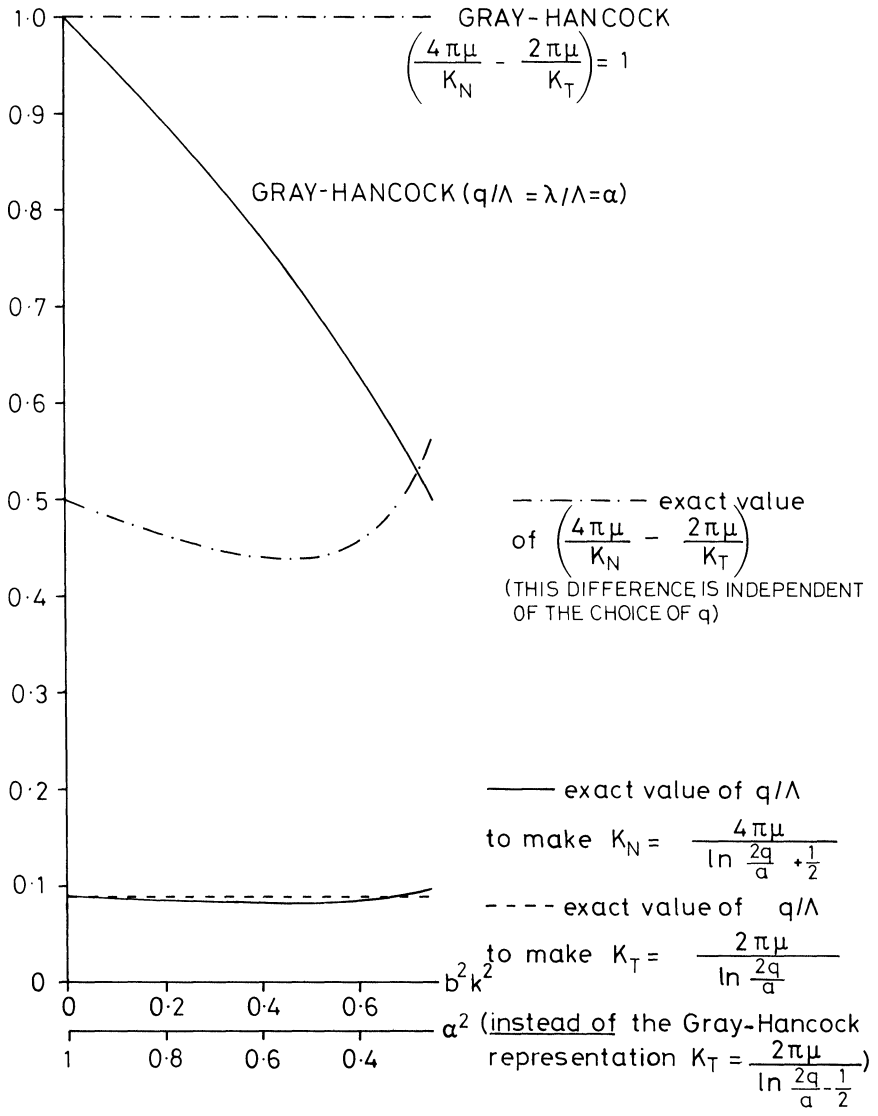

FIG. 13. *Properties of the normal resistance coefficient K_N and the tangential resistance coefficient K_T, calculated exactly for the zero-thrust swimming of spirals, are here compared with properties that were assumed by Gray and Hancock* (1955)

Lighthill (1975) assumed, after obtaining (62) with $q = 0.09\lambda$ as the value of K_N for small amplitude, that the value of K_T would necessarily be given by (61) with the same value of q, but we now see that this is not the case. Indeed, for general amplitude, the conclusions that (62) is accurate with $q = 0.09\Lambda$ and that (69) takes a value close to $\frac{1}{2}$ imply that to good accuracy

$$K_T = \frac{2\pi\mu}{\ln(2q/a)}, \tag{72}$$

with $q = 0.09\Lambda$; a formula differing from (61) in the omission of the $-\frac{1}{2}$ in the denominator. Furthermore, Fig. 13 plots (as a broken line) the value

$$\frac{q}{\Lambda} = \frac{1}{2\pi} \exp\left[\alpha^2 A_1(\alpha) + (1-\alpha^2) A_2(\alpha) - 1\right] \tag{73}$$

for q which makes (72) coincide exactly with (66), and we see that it remains even closer to 0.09 than does the earlier expression (71).

As far as the numerical values of (62) and (72) are concerned, the introduction of the reduced value $q = 0.09\Lambda$ instead of the Gray–Hancock value $q = \lambda = \alpha\Lambda$ changes the denominator by a considerably larger amount (up to $-\ln(0.09) = 2.4$) than does the omission of the $-\frac{1}{2}$ (which altered (61) into (72)). Nevertheless, this omission of the $-\frac{1}{2}$ has important consequences through its effect on the dynamically significant ratio (64).

The conclusion that in a zero-thrust spiral flagellar motion the resistance coefficients take forms (62) and (72) (with $q = 0.09\Lambda$) greatly different from the Gray–Hancock values is so important that we may usefully probe further the reasons for the difference. It is easiest to dig these out of the mathematical analysis in the limiting case of small-amplitude undulations when the formulas simplify considerably. The wavelengths λ and Λ coincide in that limit when (62) and (72) become accurate with $q = 0.09\lambda$. Lighthill (1975) already explained in detail why $q = 0.09\lambda$ is the right choice either for planar or spiral undulations of small amplitude. Here we are primarily concerned with supplementing those explanations so as to elucidate fully why in addition the $-\frac{1}{2}$ term must be removed from (61) to make the tangential resistance coefficient as in (72).

Looking back to how the $-\frac{1}{2}$ term appeared in (61), we see that it corresponds to the -2 in (18), which in turn comes from the integration by parts in (17). On the other hand, its cancellation in the analysis of the spiral undulation comes from the appearance of the -1 term in (55), again derived from an integration by parts. More careful study shows that in the limit of small amplitude these two constitute one and the same integration by parts over different ranges of integration. Furthermore, if they are carried out as a single operation over the full range of integration, no integrated term appears at all.

To see this, we recall that (12) divided the field of a stokeslet into the sum of a parallel field and a radial field. These are illustrated in Fig. 14. Section 3.2 used a stokeslet distribution along the flagellar centerline whose strength

$$\mathbf{f}(s) = (0, h \sin ks, -h \cos ks) \tag{74}$$

per unit length has zero axial component. Accordingly, any x-component (axial) of velocity cannot be part of the *parallel* field associated with the stokeslet (74). It must come entirely from its radial field, whose axial component can, according to (12), be written

$$\frac{(\mathbf{F}\cdot\mathbf{r})}{8\pi\mu}\frac{x-X}{r^3} = \frac{(\mathbf{F}\cdot\mathbf{r})}{8\pi\mu}\frac{\partial}{\partial X}\left(\frac{1}{r}\right). \tag{75}$$

Here $\mathbf{r}$ denotes displacement from a stokeslet $\mathbf{F}$ whose position has x-coordinate X. In the application to a distribution of stokeslets (74) along a flagellar centerline

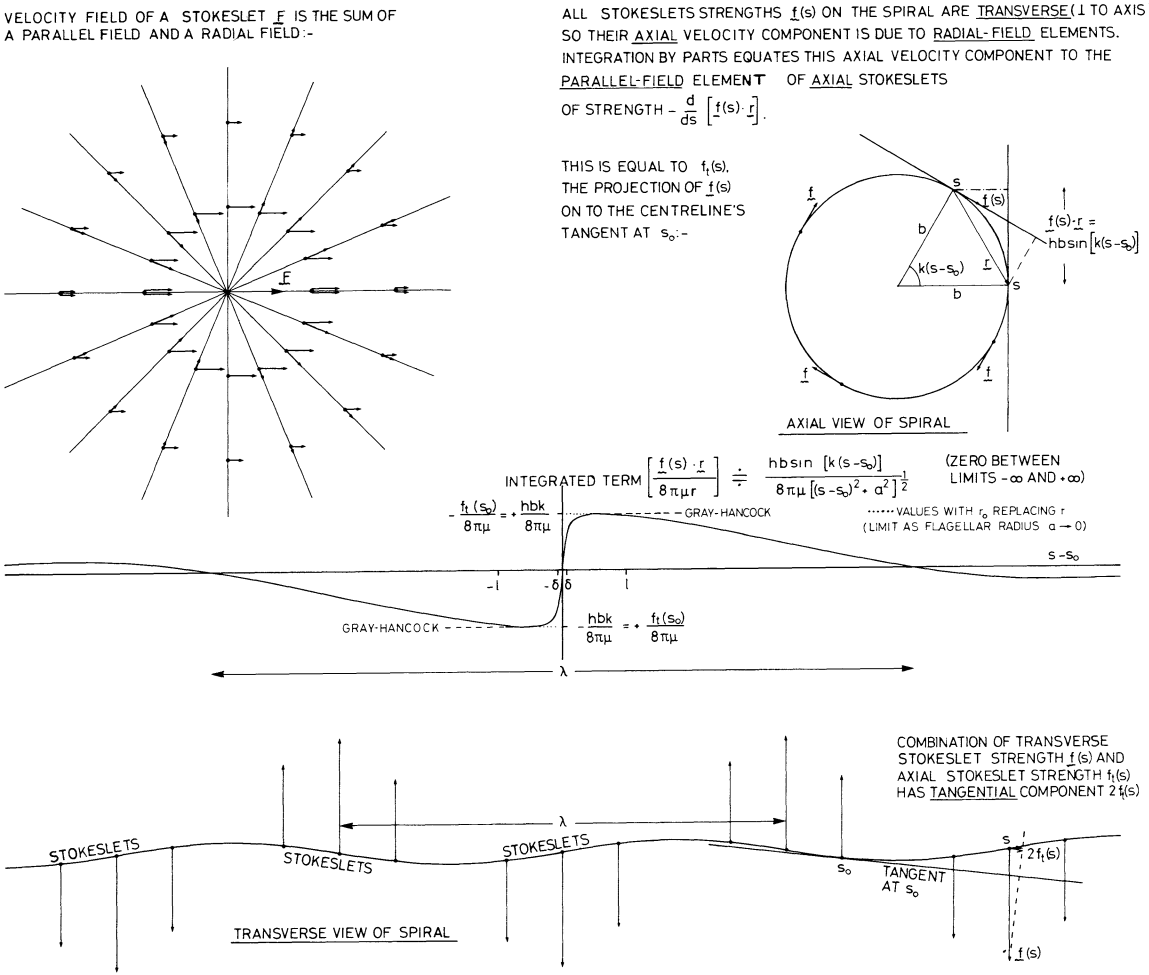

FIG. 14. *Illustrating for the small-amplitude case why in the Gray–Hancock form* (61) *of the tangential resistance coefficient the* $(-\frac{1}{2})$ *term (derived from an integration by parts) should be missing*

(33) with $X = \alpha s$, and small amplitude b, the $\partial/\partial X$ can here be replaced, with a small relative error in the limit $b \to 0$, $\alpha \to 1$, by d/ds. The associated axial velocity distribution then becomes, on integration by parts,

$$(76) \qquad \int_{-\infty}^{\infty} \frac{\mathbf{f}(s)\cdot\mathbf{r}}{8\pi\mu}\frac{d}{ds}\left(\frac{1}{r}\right)ds = \left[\frac{\mathbf{f}(s)\cdot\mathbf{r}}{8\pi\mu}\frac{1}{r}\right]_{-\infty}^{\infty} - \int_{-\infty}^{\infty} \frac{d[\mathbf{f}(s)\cdot\mathbf{r}]/ds}{8\pi\mu r}ds.$$

When we evaluate this axial velocity distribution at a point on the surface of the flagellum, we find that the integration by parts (76) effectively combines *both* the integration by parts (17) in the proof of Theorem 1 *and* the subsequent integration by parts (55) in the application of Theorem 1 to a spiral undulation. Note that the integrated term is now *zero*; indeed, since the stokeslet distribution $\mathbf{f}(s)$ has no axial component, the term $\mathbf{f}(s)\cdot\mathbf{r}$ simply oscillates between finite limits (determined, actually, in Fig. 14) while $r \to \infty$. On the other hand, its evaluation as in the proof of Theorem 1 between limits lying at a distance q, large compared with the flagellar radius a but small compared with the flagellar wavelength, would (Fig. 14) make it equal to $(-f_t/4\pi\mu)$ where f_t is the tangential component of $\mathbf{f}$. This fact was used in the proof of Theorem 1 and led to the $\sqrt{e}$ term in the value deduced for $\delta = \frac{1}{2}a\sqrt{e}$. Conversely, the application of Theorem 1 to spiral undulations involves the determination of integrals such as (76) with r replaced by the distance r_0 from a point on the flagellar centerline and with the range of integration limited to values of $r_0 > \delta$. The integrated term would then (see Fig. 14 again) have a value of $+f_t/4\pi\mu$, half contributed from each of the points where $r_0 = \delta$. When, however, we carry out the integration (76) over the full range of integration $(-\infty, \infty)$, these two expressions cancel and the total integrated term is zero.[1]

To evaluate the remaining term in the axial velocity distribution (76), we calculate, or derive geometrically as in Fig. 14, that $-d[\mathbf{f}(s)\cdot\mathbf{r}]/ds$ is the *component of* $\mathbf{f}(s)$ *along the centerline's tangent at the cross section where the velocity is being evaluated.* Note that this last term in the axial velocity distribution (76), although derived from the radial-field element in (12), has through the integration by parts acquired the same *form* as the parallel-field element of a stokeslet with an *axial* strength equal to this tangential component of $\mathbf{f}(s)$. It may be directly combined with the parallel-field element associated with the original stokeslet (transverse to the axis).

The resulting combined field (which omits only (i) the *transverse* component of the radial-field element and (ii) the field of the associated dipoles (13); fields which after cancellations are found in (79) below to yield just a *normal* velocity distribution) takes the form of the parallel-field element (only) due to a stokeslet distribution whose vector strength is the sum of the axial and transverse stokeslet strengths determined above. Those have (Fig. 14) *equal* components in the direction of the *tangent* to the centerline where the velocity is being evaluated; components adding up to *twice* the component $f_t(s)$ of $\mathbf{f}(s)$ along that tangent. The

[1] Figure 14 shows, indeed, that even when the integral is calculated over a finite range (the finite length of the flagellum), the integrated term is already small if the ends are at least half a wavelength away.

associated tangential velocity distribution is

$$\int_{-\infty}^{\infty} \frac{2f_t(s)\,ds}{8\pi\mu r}, \tag{77}$$

and in the limit of small amplitude, this is an integral of the form evaluated by Lighthill (1975, p. 52) for sinusoidally fluctuating $f_t(s)$ as

$$\begin{aligned}\frac{2f_t(s_0)}{8\pi\mu}[2K_0(ka)] &\sim \frac{f_t(s_0)}{2\pi\mu}[-\ln(\tfrac{1}{2}ka)-\gamma] \\ &= \frac{f_t(s_0)}{2\pi\mu}\ln\frac{2q}{a} \quad \text{with } q = k^{-1}e^{-\gamma} = 0.09\lambda.\end{aligned} \tag{78}$$

This confirms that it is the vanishing of the integrated term in the integration by parts (76) that brings about the replacement of the Gray–Hancock tangential resistance coefficient (61) by the improved form (72).

There is, however, no corresponding change to the form of the normal resistance coefficient (62), where the $+\frac{1}{2}$ term results from the contribution of the *dipole* distribution, exactly as in the proof of Theorem 1. The *axial* velocity distribution in the small-amplitude limit makes a contribution to normal velocity negligible compared with that of the transverse velocity distribution. The calculation (20) and (21) for the effect of the y-component of stokeslet strength and the corresponding calculation for the z-component remain valid for strengths varying sinusoidally with a wavelength very large compared with a and make that normal velocity distribution

$$\int_{-\infty}^{\infty} \frac{\mathbf{f}_n(s)\,ds}{8\pi\mu r} + \frac{\mathbf{f}_n(s_0)}{8\pi\mu}, \tag{79}$$

where the latter term comes as in (22) from the rapidly convergent integral of r^{-3} (with $\mathbf{f}_n(s)$ remaining close to $\mathbf{f}_n(s_0)$ where r^{-3} is significant). Expression (79), as above, becomes

$$\frac{\mathbf{f}_n(s_0)}{8\pi\mu}[2K_0(ka)+1] \sim \frac{\mathbf{f}_n(s_0)}{4\pi\mu}\left[\ln\left(\frac{2q}{a}\right)+\frac{1}{2}\right], \tag{80}$$

yielding the value (62) for the normal resistance coefficient.

The above analysis merely confirms for small amplitude what the preceding computations showed to be true for general amplitudes. I have thought it worth recording, however, because it explains the breakdown of the very plausible arguments of Gray and Hancock to the effect that, balancing the $+\frac{1}{2}$ in the normal resistance coefficients, a $-\frac{1}{2}$ must be included in the tangential coefficient.

Another significant application of these small-amplitude arguments is to planar undulations, which were seen in § 2.2 to be characteristic of many flagellate motions and which are considerably harder than spiral undulations to treat in the general large-amplitude case. We find that (62) and (72) with $q = 0.09\lambda$ again give the suboptimal representation of the motion by resistance coefficients, this time in the sense that they are the values needed to give the correct asymptotic forms of

the zero-thrust swimming velocity and the rate of working as the amplitude tends to zero.

Briefly, the argument goes as follows. Stokeslets of strength $(0, h \sin ks, 0)$ per unit length, distributed along a plane sinusoid $(s, b \cos ks, 0)$ of small amplitude b, make the quantity $\mathbf{f}(s) \cdot \mathbf{r}$ in (76) equal to

$$h \sin ks(b \cos ks_0 - b \cos ks). \tag{81}$$

It oscillates between finite limits, again making the integrated term zero. Minus its derivative is

$$-d[\mathbf{f}(s) \cdot \mathbf{r}]/ds = hbk(-\cos ks \cos ks_0 + \cos 2ks). \tag{82}$$

The stokeslet field which affects the tangential velocity distribution is now the sum of the *parallel-field* components (only) of axial stokeslets of strength (82) and of transverse stokeslets of strength $h \sin ks$. Its velocity component in the direction of the tangent at $(s_0, b \cos ks_0, 0)$ is

$$\begin{aligned} &\int_{-\infty}^{\infty} \frac{hbk(-\cos ks \cos ks_0 + \cos 2ks)\, ds}{8\pi\mu r} - bk \sin ks_0 \int_{-\infty}^{\infty} \frac{h \sin ks\, ds}{8\pi\mu r} \\ &= -\frac{hbk}{8\pi\mu} \int_{-\infty}^{\infty} \frac{\cos k(s - s_0)}{r}\, ds + \frac{hbk}{8\pi\mu} \int_{-\infty}^{\infty} \frac{\cos 2ks}{r}\, ds. \end{aligned} \tag{83}$$

In (83) the first term is independent of s_0 and equal to

$$-\frac{hbk}{8\pi\mu}[2K_0(ka)] \sim -\frac{hbk}{4\pi\mu} \ln \frac{2q}{a}, \tag{84}$$

with $q = 0.09\lambda$; this represents the tangential velocity's *mean value*—its only property needed for determining the swimming velocity. The mean tangential force $-\frac{1}{2}hbk$ is related to it by the resistance coefficient (72). The normal resistance coefficient, on the other hand, takes the value (62) by the same argument (79) and (80) as in the spiral case.

Note that the second integral in (83) can be expressed, taking $s - s_0$ as a new variable, as

$$\frac{hbk \cos 2ks_0}{8\pi\mu} \left(\int_{-\infty}^{\infty} \frac{\cos 2k(s - s_0)}{r}\, ds \right), \tag{85}$$

where the integral in brackets is independent of s_0, so that (85) has zero mean value as assumed above. This is one of several second-harmonic terms which are necessarily present for planar (as opposed to spiral) undulations. Kinematically, the flagellum's inextensibility requires y-components of velocity $bkc \sin ks$ to be accompanied by x-components $-U - \frac{1}{4}b^2k^2c \cos 2ks$, where U is the swimming velocity. This $\cos 2ks$ term does *not*, however, affect the *mean* tangential velocity

$$-U - \tfrac{1}{2}b^2k^2c. \tag{86}$$

Finally, second-harmonic axial forces are necessary (in addition to first-harmonic transverse forces) if the kinematically correct second-harmonic axial velocity is to

be generated; but these do not affect the mean tangential force (84), or its relation to the mean tangential velocity (86). Furthermore, these second-harmonic forces are of the second-order in amplitude so that their rate of working is negligible (of fourth order compared with the leading second order term, $\frac{1}{2}hbkc$ per unit length).

To sum up, we have shown that a suboptimal representation of zero-thrust flagellar undulations by normal and tangential resistance coefficients requires

$$K_N = \frac{4\pi\mu}{\ln(2q/a)+\frac{1}{2}}, \quad K_T = \frac{2\pi\mu}{\ln(2q/a)} \tag{87}$$

with $q = 0.09\Lambda$ (where Λ is wavelength measured along the flagellum) for either spiral or planar motions of small amplitude, *and also* for spiral undulations of arbitrary amplitude. In the absence of other information, it would be reasonable to use (87) also for planar undulations of arbitrary amplitude.

3.4. Superior representations of more general flagellar motions. In this section, putting aside representations of flagellar motions by resistance coefficients, I resume the study of how Theorem 1 can be used to find better representations, this time of motions more general than the zero-thrust spiral motion studied with end effects neglected in § 3.2. Two more motions are analyzed, though still with end effects largely neglected: a spiral motion as modified to give *nonzero* thrust, and then the same motion as further modified by the velocity field associated with the counterbalancing drag force on the cell body. Actually, there is a sense in which neither of these analyses can completely neglect the ends of the flagellum; certainly the conclusions, unlike those of § 3.2, depend upon its total length L. The methods do, nevertheless, involve some averaging over the length L and avoid going into details of force distribution very near the ends, thus avoiding complications associated with the kinematics of the basal region of a flagellum where it is attached to the cell body, or any vagaries of flagellar tip movements.

I already indicated in § 3.2 how the theory of spiral motions would have to be modified to apply to motions with nonzero thrust. A flagellar motion generating a mean thrust per unit length g in the *negative* x-direction exerts on the fluid an equal and opposite mean force $(+g, 0, 0)$ per unit length. A distribution along the spiral (33) of stokeslets with a nonzero mean $(g, 0, 0)$ and the right invariance properties was written down in (43). Then, however, Theorem 1 was applied to this distribution, in (48), only in the case $g = 0$. Now we determine what extra velocity field must be added to the right-hand side of (48) when the extra constant value $(g, 0, 0)$ is added on to the stokeslet strength.

This extra stokeslet strength $\Delta\mathbf{f}(s) = (g, 0, 0)$ per unit length has tangential component $g\alpha$ by equation (35). The associated vector $\Delta\mathbf{f}_n(s)$ normal to the centerline referred to in Theorem 1 is obtained by subtracting from $\Delta\mathbf{f}(s)$ its tangential resultant to give

$$\begin{aligned}\Delta\mathbf{f}_n(s) &= \Delta\mathbf{f}(s) - g\alpha(\alpha, -bk\sin ks, bk\cos ks)\\ &= gbk(bk, \alpha\sin ks, -\alpha\cos ks).\end{aligned} \tag{88}$$

Theorem 1 then gives the extra flagellar velocity $\Delta\mathbf{w}$ at $s_0 = 0$ associated with this $\Delta\mathbf{f}(s)$ as

$$\Delta\mathbf{w} = \frac{gbk}{4\pi\mu}(bk, 0, -\alpha) + \int_{r_0>\delta} \frac{r_0^2(g, 0, 0) - (g\alpha s)\mathbf{r}_0}{8\pi\mu r_0^3}\, ds \tag{89}$$

with $\mathbf{r}_0$ as in (49).

Although the integral in (48) was evaluated between the limits $s = -\infty$ and $s = +\infty$ in order to estimate $\mathbf{w}$ at $s = 0$ with end effects neglected, a modified procedure is needed for the integral in (89), which does not converge as $|s| \to \infty$. We evaluate it between limits $-s_1$ and $+s_2$, representing the ends of the flagellum, and express the "neglect of end effects" only in the assumption that

$$\theta_1 = ks_1 \quad \text{and} \quad \theta_2 = ks_2 \tag{90}$$

are both very large.

The x-component of (89) involves an integral

$$\int_{r_0>\delta} \frac{ds}{r_0} = \left(\int_{-s_1}^{-\delta} + \int_{\delta}^{s_2}\right)\frac{ds}{r_0} = \left(\int_{-\theta_1}^{-\varepsilon} + \int_{\varepsilon}^{\theta_2}\right)\frac{d\theta}{[\alpha^2\theta^2 + 2(1-\alpha^2)(1-\cos\theta)]^{1/2}}. \tag{91}$$

The integrand in (91) behaves like $|\theta|^{-1}$ as $|\theta| \to 0$ but like $\alpha^{-1}|\theta|^{-1}$ as $|\theta| \to \infty$, so that the integral can be written for large θ_1 and θ_2 and small ε as

$$\alpha^{-1} \ln(\theta_1\, \theta_2) - 2\ln\varepsilon - 2A_3(\alpha), \tag{92}$$

where the function $A_3(\alpha)$ (independent of θ_1, θ_2 and ε) is easy to compute and is plotted in Fig. 15.

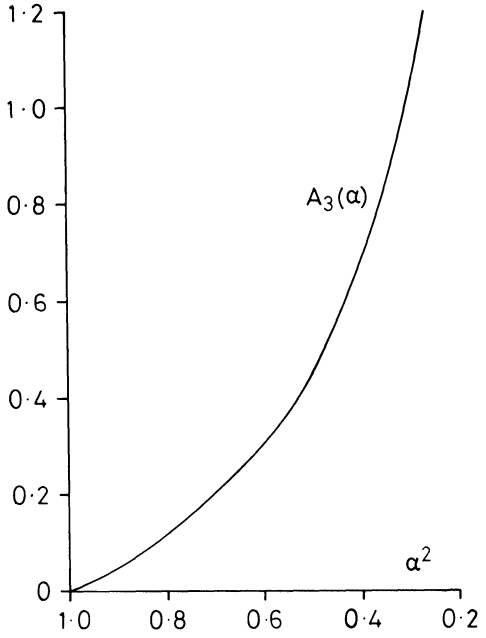

FIG. 15. *The function $A_3(\alpha)$ defined in* (92)

Note also that expression (91), on integration by parts, becomes

$$(93)\qquad \left[\frac{\theta}{[\alpha^2\theta^2+2(1-\alpha^2)(1-\cos\theta)]^{1/2}}\right]+\int\frac{\theta[\alpha^2\theta+(1-\alpha^2)\sin\theta]\,d\theta}{[\alpha^2\theta^2+2(1-\alpha^2)(1-\cos\theta)]^{3/2}}$$

taken between the same two pairs of limits. We can use the function $A_1(\alpha)$ defined in (53) to express part of the integral in (93): the part involving $\theta\sin\theta$ which converges as $|\theta|\to\infty$. It follows by equating (92) and (93) for large θ_1 and θ_2 that the other part can be written

$$(94)\qquad \left(\int_{-\theta_1}^{-\varepsilon}+\int_{\varepsilon}^{\theta_2}\right)\frac{\alpha^2\theta^2\,d\theta}{[\alpha^2\theta^2+2(1-\alpha^2)(1-\cos\theta)]^{3/2}}$$
$$=\alpha^{-1}\ln(\theta_1\theta_2)-2\alpha^2\ln\varepsilon-2[A_3(\alpha)+(1-\alpha^2)A_1(\alpha)+\alpha^{-1}-1],$$

a result which allows (89) to be evaluated in terms of the computed functions $A_1(\alpha)$ and $A_3(\alpha)$ only.

Equation (89) specifies the change $\Delta\mathbf{w}$, due to a mean thrust g per unit length, in the value of $\mathbf{w}$ at $s=0$ given by (41). This implies a change $\Delta U=U-U_0$ in the swimming speed U from its zero-thrust value U_0, and a corresponding change $\Delta\omega_E$, given by the x- and z-components of (89) as

$$(95)\qquad \begin{aligned}4\pi\mu(\Delta U)&=-g[1-\alpha^2+\alpha^{-1}\ln(\theta_1\,\theta_2)-(1+\alpha^2)\ln\varepsilon\\&\qquad -2A_3(\alpha)-(1-\alpha^2)A_1(\alpha)-\alpha^{-1}+1],\\4\pi\mu(\Delta\omega_E)b&=-g\alpha bk[-1-\ln\varepsilon+A_1(\alpha)],\end{aligned}$$

equations that supplement (56) in the case $g\neq 0$.

Strictly speaking, the quantity $\ln(\theta_1\,\theta_2)$ appearing in the expression (95) for ΔU is not independent of the choice of origin—that is, the choice of position $s_0=0$ along the flagellum where ΔU is being evaluated. However, in a spiral of total length L, the value of $\ln(\theta_1\theta_2)$ when the origin lies at a distance σL from one tip (where $0<\sigma<1$) is

$$(96)\qquad 2\ln(kL)+\ln[\sigma(1-\sigma)],$$

whose value averaged with respect to σ is

$$(97)\qquad \langle\ln(\theta_1\,\theta_2)\rangle=2\ln(kL)-2.$$

Note that the exact expression (96) remains within ± 0.6 of the average expression (97) whenever $0.07<\sigma<0.93$. As that amount of variation is unimportant in (95) when compared with the large terms proportional to $\ln(kL)$ and $-\ln\varepsilon$, we assume that $\ln(\theta_1\,\theta_2)$ can to adequate approximation be replaced by the averaged value (96) in a theory that does not attempt to investigate end effects. This assumption is later checked in a particular case.

We calculate the quantitative implications of the above theory when the flagellar thrust has to balance a cell body drag $6\pi\mu UA$. Here A is defined as the *radius of a sphere with the same drag as the cell body*, and we briefly postpone consideration of any interaction between the flow fields associated with flagellar

thrust and cell body drag. Thus we simply take the thrust per unit length of flagellum in the above analysis as

$$g = 6\pi\mu UA/L. \tag{98}$$

The total swimming velocity U can now be written as a sum of terms from (56) and (95), where g is replaced in terms of this total U itself by (98). This gives

$$4\pi\mu U = h\alpha bk[-1-\ln\varepsilon + A_1(\alpha)](1+\Psi A/L)^{-1}, \tag{99}$$

where the nondimensional factor

$$\Psi = \tfrac{3}{2}[2-\alpha^2-3\alpha^{-1}+2\alpha^{-1}\ln(kL)-(1+\alpha^2)\ln\varepsilon-2A_3(\alpha) \\ -(1-\alpha^2)A_1(\alpha)] \tag{100}$$

is plotted in Fig. 16. Similarly the total effective angular velocity ω_E can be written

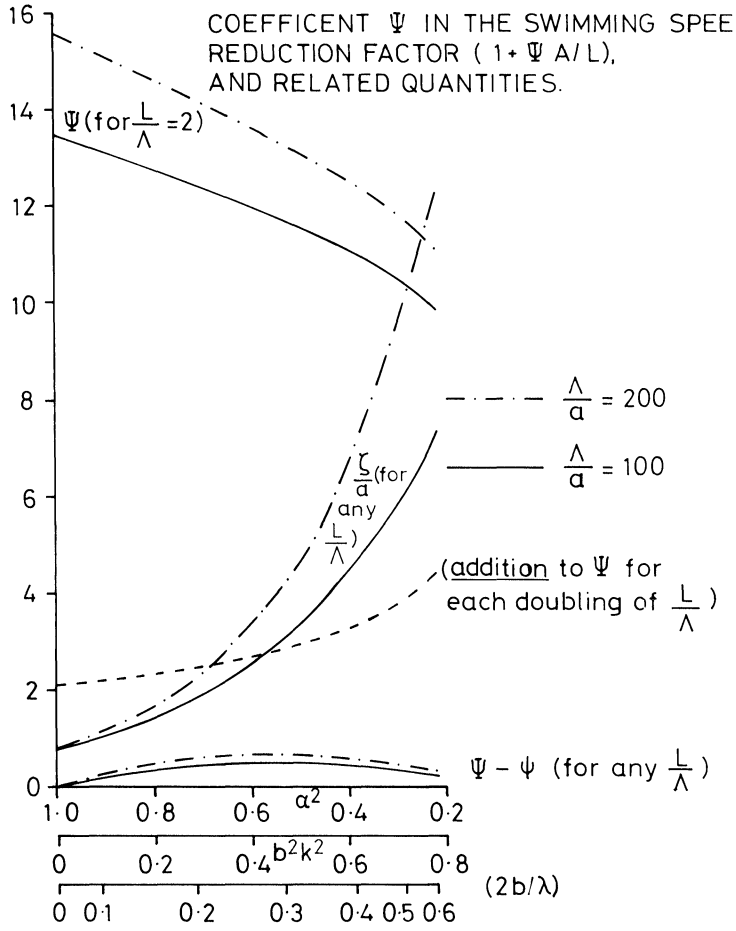

FIG. 16. *Thrusting motion of spiral flagella*

as the sum of terms from (56) and (95), with g replaced in terms of h by (98) and (99), to give

$$4\pi\mu\omega_E b = h[-(1-\alpha^2)-(2-\alpha^2)\ln\varepsilon+\alpha^2 A_1(\alpha) + 2(1-\alpha^2)A_2(\alpha)]\frac{1+\psi A/L}{1+\Psi A/L}, \tag{101}$$

where

$$\Psi-\psi=\frac{\frac{3}{2}\alpha^2(1-\alpha^2)[-1-\ln\varepsilon+A_1(\alpha)]^2}{[-(1-\alpha^2)-(2-\alpha^2)\ln\varepsilon+\alpha^2 A_1(\alpha)+2(1-\alpha^2)A_2(\alpha)]} \tag{102}$$

is also plotted in Fig. 16. (For the quantity ζ additionally plotted in Fig. 16, see (110) below.)

Figure 16 essentially sums up all the information we need for comparing nonzero-thrust spiral motions with the zero-thrust spiral motions described in Fig. 12. Thus it follows from (99) and (101) that values of U/V_E (ratio of swimming speed U to apparent wave velocity $V_E=\alpha\omega_E/k$), of $E/\mu U^2$ (where E is rate of working per unit length of flagellum), and of χ (the nondimensional form defined in (59) of the moment of the spiral flagellum) are *changed from their zero-thrust values by the following factors*:

$$\begin{aligned} U/V_E &\quad \text{changed by factor} \quad (1+\psi A/L)^{-1}; \\ E/\mu U^2 &\quad \text{changed by factor} \quad (1+\Psi A/L)(1+\psi A/L); \\ \chi &\quad \text{changed by factor} \quad (1+\Psi A/L)(1+\psi A/L)^{-1}. \end{aligned} \tag{103}$$

Evidently, the changes depend very critically on A/L; they are greatest for the rate-of-working factor $E/\mu U^2$, substantial for the swimming-speed ratio U/V_E, and insignificant (since $\Psi-\psi$ is very much smaller than Ψ itself) for the moment ratio χ. Actually, the fact (Fig. 16) that $\Psi-\psi$ is everywhere less than 0.05Ψ means that to close approximation, the changes result exclusively from the change (99) in U alone, *dividing* the ratio U/V_E by one factor $1+\Psi A/L$, and *multiplying* $E/\mu U^2$ by two such factors.

The psi coefficients in these nonzero-thrust correction factors $1+\Psi A/L$ are seen in Fig. 16 to take values in the region 10 to 15, considerably greater than the values around 5 obtained by use of the same resistance coefficients as for evaluation of the zero-thrust swimming speed (see, for example, Lighthill (1975, p. 55)). Indeed, the whole idea of a local resistance coefficient is peculiarly inappropriate to the evaluation of this change in swimming velocity due to a distribution of thrust all along the flagellum. Whereas in the zero-thrust case there is cooperative application of force from within a certain radius 0.09Λ of any given point, but the effects of the fluctuating forces further from the point essentially cancel, no such localization of the effects of a uniform distribution of thrusting forces can be expected; they exercise coooperative action all along the flagellum. This brings about a considerably greater change in swimming velocity than would be predicted from the high values of resistance coefficients associated (§ 3.3) with the analysis of the zero-thrust case.

To anyone who, in spite of the above considerations, may nevertheless seek a treatment in terms of resistance coefficients, the following *very* crude approach may be suggested. A single special "axial resistance coefficient" may be used to determine the nonzero-thrust correction to swinming speed. This resistance coefficient K_X is defined as the ratio of thrust per unit length to the resulting swimming-speed reduction

$$K_X = g/(-\Delta U) = 6\pi\mu/\Psi. \tag{104}$$

The idea is that an organism swimming at velocity $U < U_0$ is essentially imposing on the undulating spiral an effective *motion in the opposite direction* at velocity $U_0 - U = -\Delta U$ *relative to its natural zero-thrust motion.* The resistance $K_X(-\Delta U)$ to that provides a thrust g per unit length which balances the drag resisting the forward movement of the cell body.

With this background, it is interesting that the values of Ψ calculated in Fig. 16 enable us to express K_X in the form

$$K_X = \frac{2\pi\mu}{\ln(2q/a)} \tag{105}$$

used for tangential resistance coefficients in § 3.3, and that the q so calculated is related as in Fig. 17 to the component $l = \alpha L$ of the flagellum's length in the

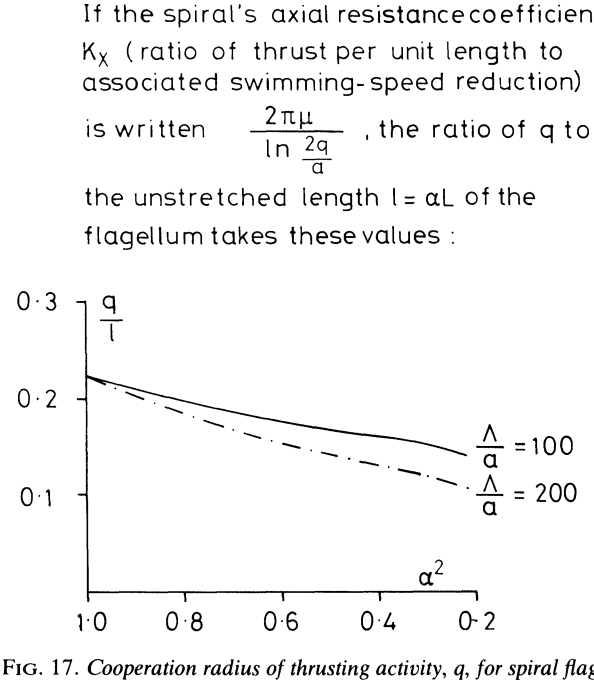

FIG. 17. *Cooperation radius of thrusting activity, q, for spiral flagella*

direction of propagation, that is, the distance within which the thrusting forces act cooperatively. The ratio q/l take the value

$$q/l = e^{-3/2} = 0.22 \tag{106}$$

for $\alpha = 1$, and values rather smaller than that for other values of α. A value around $q = \frac{1}{6}l$ is found for values of α giving high-efficiency spiral motions (cf. Fig. 12), suggesting that sufficient accuracy in very crude calculations may be obtained by using (104) and (105) with $q = \frac{1}{6}l$ as a typical radius of cooperative thrusting action. This approximation leads to a reduction factor

$$(1+\Psi A/L)^{-1} \quad \text{with} \quad \Psi \doteqdot 3[\ln (l/3a)]^{-1} \tag{107}$$

on the swimming velocity of a cell body with drag $6\pi\mu UA$.

There is just one case when the above values of K_X may be related to accurately known quantities. In the limit $\alpha \to 1$, K_X tends to the tangential resistance coefficient for a straight cylinder of length L and radius a. This quantity has been known for some time (Cox (1970, p. 805)) to take the value given by (105) and (106). This confirms the above method based on using an *average* value (97) for $\ln(\theta_1\,\theta_2)$ (whereas a "Gray–Hancock" approach, assigning to $\ln(\theta_1\,\theta_2)$ its *maximum* value $2\ln(\frac{1}{2}kL)$ attained at $\sigma = \frac{1}{2}$, would incorrectly give q/l the value $\frac{1}{2}e^{-1/2} = 0.30$).

Another, really more useful, representation of the expression (95) for the change ΔU in swimming speed is suggested when we recognize that the thrust g per unit length generating that change corresponds to a *thrust* $g\alpha^{-1}$ *per unit axial distance*. This is because by (33) the axial separation of the stokeslet s from the cross section $s = 0$ is

$$X = \alpha s. \tag{108}$$

The inverse-first-power dependence on X of the effect of axial stokeslets of strength $g\alpha^{-1}$ per unit axial distance on the axial velocity at $X = 0$ is asymptotically

$$\frac{g\alpha^{-1}\,dX}{4\pi\mu|X|}, \tag{109}$$

which on integration to large values of $|X|$ leads to the term $-g\alpha^{-1}\ln(\theta_1\,\theta_2)$ in the expression (95) for $4\pi\mu(\Delta U)$. This suggests that we seek to express the exact expression (95) as

$$4\pi\mu(\Delta U) = -\left(\int_{-X_1}^{-\zeta} + \int_{\zeta}^{X_2}\right)\frac{g\alpha^{-1}\,dX}{|X|} \tag{110}$$

where $X_1 = \alpha s_1$, $X_2 = \alpha s_2$, and the value of ζ such that (110) coincides with (95) is easily computed and is plotted in Fig. 16.

Equation (110) states that the excess swimming speed at the cross section $X = 0$ due to axial stokeslets $g\alpha^{-1}$ per unit axial distance distributed along the spiral is exactly equal to the solution of a much simpler problem: determine the excess swimming speed *on the axis of the spiral* resulting from the *same* stokeslets distributed along all parts of the axis except those within a small distance ζ of the origin. All the complicated local effects of the spiral geometry are here represented through ζ, which has been calculated exactly—whereas interactions over longer distances (comparable with a wavelength) are well represented by the simple asymptotic velocity field (109).

These ideas suggest a method for estimating the effect of a thrust per unit length which may *vary* slowly along a spiral flagellum. We assume that it generates an axial velocity field given by (109), associated with stokeslets of strengths $g\alpha^{-1}$ per unit axial distance distributed along the axis of the spiral, but with the velocity at any cross section equal to the resulting velocity on the axis determined by ignoring stokeslets within an axial distance ζ. This assumption should give a good approximation because (109) should be accurate at larger distances while, if g is varying slowly, the local effects of the spiral geometry may be well represented by the form obtained as in (110) by taking g constant. In this case, then, (110) may be used with $g = g(X)$.

We illustrate the above ideas by applying them tentatively to estimate the effects of mutual interaction between flagellar thrust and cell body drag, in the special case of a spherical cell body of radius A propelled by a spiral flagellum of length L much greater than A. Then it is convenient to relocate the origin of x at the join between the two, with the center of the sphere at $x = -A$ and the spiral extending from $x = 0$ to $x = l$, where

$$l = \alpha L \tag{111}$$

is the unstretched length of the spiral. (The same analysis applies whether we are dealing with a posterior flagellum in base-to-tip undulations or an anterior flagellum in tip-to-base undulations.)

This is a case when some significant variation in $T(X)$, the thrust per unit axial distance (replacing $g\alpha^{-1}$ in the above analysis), must be expected; particularly, an increase near the cell body, which tends to drag nearby fluid along with it requiring the flagellum locally to exert increased thrust. The drag D on the cell body must be balanced by the total thrust:

$$D = \int_0^l T(X)\, dX. \tag{112}$$

Conversely, the cell body moves at swimming velocity U through a fluid which is being induced to move in the opposite direction by the thrust of the flagellum. Using the induced velocity at the center of the sphere as an estimate of this effect, we obtain

$$D = 6\pi\mu A\left[U + \int_0^l \frac{T(X)\, dX}{4\pi\mu(A+X)}\right] \tag{113}$$

as an estimate of the resulting increased drag.

Finally, we must write down the axial velocity $-U$ at the position $x = X_0$ of the flagellum as a sum of (i) the value of $-U_0$ (where U_0 is the zero-thrust swimming speed); (ii) the effect of a stokeslet of strength $-D$ situated at the sphere's center $x = -A$; (iii) the effect of the distribution of thrust $T(X)$; as

$$-U = -U_0 - \frac{D}{4\pi\mu(A+X_0)} + \left(\int_0^{X_0-\zeta} + \int_{X_0+\zeta}^{l}\right)\frac{T(X)\, dX}{4\pi\mu|X-X_0|}. \tag{114}$$

Here the formula (110) for velocity field due to thrust has been modified by choosing a new origin (so that the velocity field is written down now at $x = X_0$) and

by replacing $g\alpha^{-1}$ by $T(X)$. Equation (114) must hold for each X_0 (although we neglect end effects and do not seek answers for X_0 very close to 0 or l); thus it is an integral equation for $T(X)$ which must be satisfied for some constant values of U and D which in turn must satisfy (112) and (113).

To the same approximation as was made in the first half of this section, with a logarithmic term replaced by its average as in (97), the solution is quite easily obtained in the form

$$T(X) = B + \frac{C}{A+X}. \tag{115}$$

Substituted in (114), this gives

$$4\pi\mu(U_0 - U) + \frac{D}{A+X_0} = \left(B + \frac{C}{A+X_0}\right) \ln \frac{X_0(l-X_0)}{\zeta^2} + \frac{C}{A+X_0} \ln \frac{(X_0+A)^2 - \zeta^2}{A(l+A)}. \tag{116}$$

The right-hand side of (116) is approximated by replacing $\ln[X_0(l-X)]$ by its average

$$2 \ln l - 2 \tag{117}$$

as in (97), and similarly replacing $\ln[(X_0+A)^2 - \zeta^2]$ by the average in $0 < X_0 < l$ of its value with the small ζ^2 term neglected:

$$\frac{1}{l}\int_0^l \ln[(X_0+a)^2]\, dX_0 = \frac{2}{l}[(l+A)\ln(l+A) - A \ln A - l], \tag{118}$$

which for A much smaller than l takes the same value (117). Equation (116) then becomes

$$4\pi\mu(U_0 - U) + \frac{D}{A+X_0} = \left(B + \frac{C}{A+X_0}\right)\left(2\ln\frac{l}{\zeta} - 2\right) + \frac{C}{A+X_0}\left(\ln\frac{l}{A} - 2\right), \tag{119}$$

which is satisfied if the constants B and C satisfy

$$4\pi\mu(U_0 - U) = 2B\left(\ln\frac{l}{\zeta} - 1\right), \qquad D = C\left(2\ln\frac{l}{\zeta} + \ln\frac{l}{A} - 4\right). \tag{120}$$

In the meantime, the solution (115) makes (112) and (113) become

$$D = Bl + C\ln\frac{l}{A}, \qquad D = 6\pi\mu AU + \tfrac{3}{2}A\left(B\ln\frac{l}{A} + \frac{C}{A}\right). \tag{121}$$

These four equations for the unknowns B, C, D and U are readily solved. From the second and third of them, the relationship between the coefficients B and C takes the simple form

$$Bl = 2C\left(\ln\frac{l}{\zeta} - 2\right). \tag{122}$$

The third and fourth equations then give the relation between B and U (again with A taken much smaller than l) as

$$Bl\left[1 + \frac{\ln(l/A) - \frac{3}{2}}{2(\ln(l/\zeta) - 2)}\right] = 6\pi\mu AU. \tag{123}$$

The first equation then gives the swimming speed as

$$U = U_0 \Big/ \left\{1 + \left[\frac{3A}{l}\left(\ln\frac{l}{\zeta} - 1\right)\right]\left[1 + \frac{\ln(l/A) - \frac{3}{2}}{2(\ln(l/\zeta) - 2)}\right]^{-1}\right\}. \tag{124}$$

Note that in (124) the first square bracket is *exactly* the value $(\Psi A/L)$ given in (99) by the theory with flow field interactions between flagellum and cell body neglected, as the definition of ζ implies. Accordingly, in the factor $(1+\Psi A/L)$ by which the swimming speed U is reduced below the zero-thrust value U_0 as a result of the thrust needed to balance the drag on a cell body of radius A, *consideration of flow field interactions has the effect of lowering the value of* Ψ through division by

$$\left[1 + \frac{\ln(l/A) - \frac{3}{2}}{2(\ln(l/\zeta) - 2)}\right]. \tag{125}$$

Values of this factor, which are easily obtained from the values of ζ given in Fig. 16, are in typical cases a little less than 1.5, producing a significant but not overwhelming lowering of the value of Ψ; that is, a lowering in the extent of the reduction of swimming velocity due to cell body drag.

3.5. Flow fields generated by flagella. An account of flagellar hydrodynamics should go beyond the calculation of relationships between flagellar movements in fluid and the associated forces, and beyond the estimation of hydrodynamic effects on microorganism locomotion, to study also the fluid *flow fields generated by flagella*, with their special significance not so much for locomotion as for feeding. In this attempt to initiate hydrodynamic studies of flagellar motions, therefore, I include a section on flow fields and their relevance to the feeding problems of microorganisms, although I limit the discussion to one extreme case only: the case of sessile organisms, for which locomotion is altogether absent. The entire function of flagellar thrust is then to generate a flow field for feeding purposes, that thrust being balanced by an equal and opposite reaction from a stalk which attaches the organism to a substrate (§ 2.2).

I estimate the flow field in this case partly because it is an extreme case of very definite interest and partly because it is one which avoids the particular complication investigated at the end of § 3.4: there is no motion of the cell body through the fluid contributing to the forces driving the fluid motion.

Actually, the study of this flow field illustrates rather well the power of the method of §§ 3.2 and 3.4 based on first determining the zero-thrust swimming speed U_0 and then the change $\Delta U = U - U_0$ in swimming speed associated with a given thrust g per unit length. Evidently, the sessile case requires $U = 0$, which implies that $\Delta U = -U_0$. In the notation of the axial resistance coefficient K_X defined by equation (104), this implies a thrust per unit length

$$g = K_X U_0. \tag{126}$$

Thus the flagellar thrust, generated when a sessile organism makes given flagellar undulations, may be simply written down in terms of (i) the zero-thrust swimming speed associated with the same undulations and (ii) the axial resistance coefficent K_X associated with the flagellar configuration. For example, if the flagellar undulations took the form of a spiral of constant radius and constant

pitch, the expression (126) could be immediately evaluated from the values of U_0 given in Fig. 12 and the values of $\Psi = 6\pi\mu/K_X$ given in Fig. 16.

Actually, it is doubtful whether any sessile organisms make use of spiral undulation. Evidently, this would be impossible unless the organism's attachment to the substrate had enough torsional strength to balance the hydrodynamic moment. Planar undulations are common, however. Accordingly, it may be desirable here to indicate how the thrust per unit length g would be estimated for planar undulations. In fact, this illustrates well the utility of suboptimal representations by resistance coefficients in problems where calculations of superior accuracy have not yet been done.

First, we may estimate the zero-thrust swimming speed U_0, even (see the end of § 3.3) for planar undulations of arbitrary amplitude, by using the resistance coefficients (87) with $q = 0.09\Lambda$ (where Λ is curvilinear wavelength). Their ratio is

$$r_K = K_T/K_N = \frac{1}{2} + \frac{1}{4}\left(\ln\frac{2q}{a}\right)^{-1}. \tag{127}$$

It is known (Lighthill (1975, Chap. 3)) that analysis of planar undulations by use of resistance coefficients gives a value

$$\frac{U_0}{V} = \frac{(1-\beta)(1-r_K)}{1-\beta+r_K\beta} \tag{128}$$

in terms of r_K and of β, the *mean square cosine* of the angle between the flagellar tangent and the swimming direction.

While for the zero-thrust case we use these results with a small value $q = 0.09\Lambda$ for the "cooperation radius" of thrusting activity, we estimate the other factor in (126) differently. Because (§ 3.4) the axial resistance coefficient K_X relates the distribution of thrust g along the flagellum to the change in swimming speed it produces, a "cooperation radius" proportion to the axial extent l of the thrust distribution is appropriate, and we accordingly choose K_X as in (105), taking a value of q around $\frac{1}{6}l$ as suggested by Fig. 17.

Note that the associated rate of working is the same as when the same undulations produce zero-thrust swimming. This is because (i) a *zero-thrust* system of forces does work at the same rate after a uniform axial velocity is superimposed, and (ii) a uniform thrust per unit length g does no work in a motion with zero mean axial velocity.

The large-scale flow field generated by the flagellar motions is primarily that of the thrust distribution (126). The reasons for this is that *zero-thrust* flow fields have a *small-scale* character, extending a distance of considerably less than a wavelength from the flagellum. This can be seen mathematically from the fact that solutions of the Stokes equations (1) and (2) which vary sinusoidally in the x-direction like $\exp(2\pi ix/\lambda)$ decay exponentially with distance $(y^2+z^2)^{1/2}$ from the x-axis, roughly like

$$\exp[-2\pi(y^2+z^2)^{1/2}/\lambda]. \tag{129}$$

In other words, the associated flow fields are merely *local.* Experimental confirmation of this for zero-thrust swimming of a nematode worm by planar undulations is given in Fig. 18, a flow visualization due to Gray (1968).

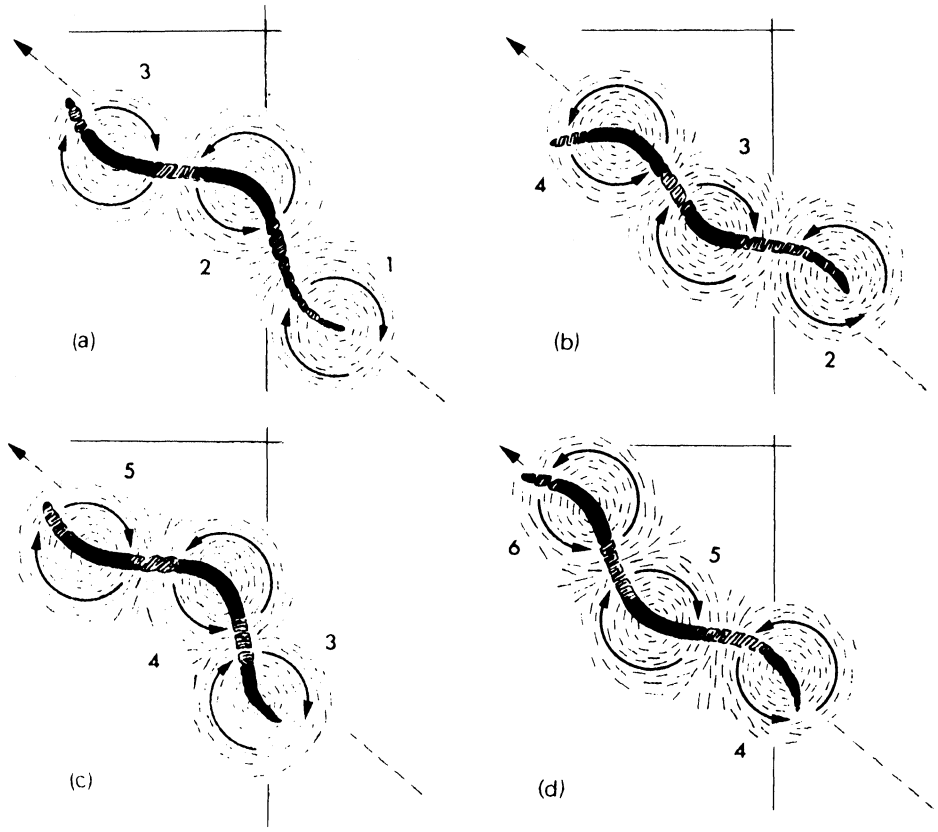

FIG. 18. *Flow visualization (Gray (1968)) of the pattern of streamlines in the neighborhood of a swimming nematode worm Turbatrix. Undulatory locomotion of such an organism is a true zero-thrust swimming since there is no separate drag element to be propelled*

This suggests that the large-scale flow field can be represented along the lines suggested near the end of § 3.4 by means of a simple *uniform distribution along the axis*

$$T = gL/l \tag{130}$$

of thrust per unit axial distance, where L and l are the flagellum's stretched and unstretched lengths. This is because the *difference* between the complicated real distribution of force on the fluid and that simple uniform distribution of thrust along the axis is a zero-thrust distribution, which generates merely a small-scale localized flow field.

Now, the streamlines associated with a uniform axial distribution of force T per unit length along an axial segment of length l are easy to compute and are displayed in Fig. 19. The flow field has axial symmetry of course; it also has fore-and-aft symmetry about the segment's midpoint. The streamlines are the same whether the flagellum is thrusting to the right or to the left, the *flow* being in the direction opposite to the thrust. For the smooth flagella here considered, then, the flow would be in the direction of propagation of the undulation.

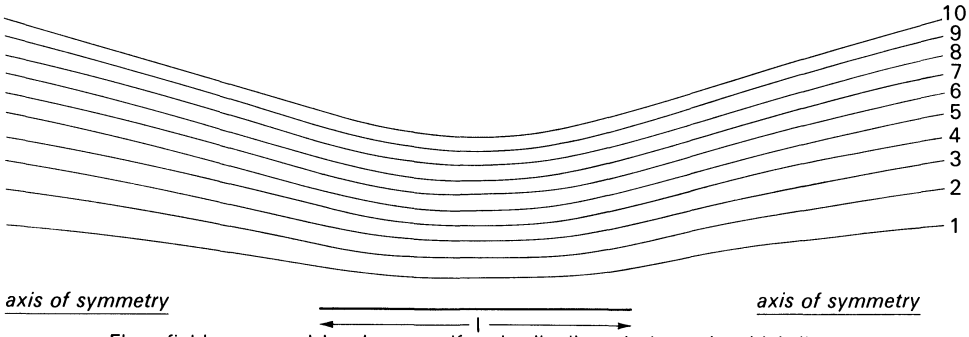

FIG. 19. *Approximate flow field generated by the flagellum of a sessile organism*

The streamlines in Fig. 19 are meridian sections of stream-tubes enclosing volume flow rates of fluid taking values which are integer multiples (from 1 to 10) of a flow rate $0.0125Tl^2/\mu$. Thus, when the diagram is rotated about the axis of symmetry, there is equal flow rate in each of the annular regions between the tubes. Note that, since the thicknesses of these regions show little variation with distance from the axis, their cross-sectional areas should increase linearly with that distance, consistently with the flow velocity falling off as an inverse-first-power of that distance.

The calculation neglects, of course, any interference with the flow field due to the presence of the cell body, or of a "collar" of fine pseudopodia filtering the flow as in choanoflagellates, or of a cup-shaped lorica to which the cell body may be attached. These, however, are obstacles of relatively modest scale which may only slightly deform the flow field. By contrast, if there were a plane solid substrate close to the flow of Fig. 19, a very considerable deformation would be induced. This could be represented (Blake (1971)) by an image system in the solid wall, consisting predominantly of equal and opposite stokeslets at the mirror-image positions. Those would reduce the flow of Fig. 19 considerably if the wall were close by.

This argument makes evident the important role of the *stalk* in those sessile microorganisms that generate flows for feeding purposes by flagellar motions. The flows generated would be considerably reduced were it not for the fact that the stalk allows the flagellum to operate well clear of where the solid substrate can interfere significantly with its flow field. Mathematically, the stalk ensures that the image stokeslets remain at a distance from the flagellum of over twice the length of the stalk and lorica combined.

It is worth asking what type of flagellar motion requires least rate of working to generate a given volume flow through a *disc of radius R* at the base of the flagellum (representing, for example, the "collar" of a choanoflagellate). The calculations leading to Fig. 19 show that flow rate to be

$$Q = \frac{TR^2}{4\mu} \sinh^{-1}\left(\frac{l}{R}\right) \doteqdot \frac{TR^2}{4\mu} \ln \frac{2l}{R}. \tag{131}$$

Now (130) allows T to be written $g\alpha^{-1}$, where for general planar undulations $\alpha = l/L$ is the *mean value* of that cosine of the angle between the flagellar tangent and the axis whose *mean square* is β. With (126), this gives

$$Q = \alpha^{-1} U_0 R^2 \left(\frac{K_X}{4\mu} \ln \frac{2l}{R}\right). \tag{132}$$

On the other hand, the rate of working by the flagellum was shown earlier to be the same as for zero-thrust swimming at velocity U_0. This rate of working is known (Lighthill (1975, pp. 59, 60) with zero substituted for his parameter δ) to take the value

$$K_T L U_0^2 (1 - r_K)^{-2} (1 - \beta)^{-2} (1 - \beta + r_K \beta)[\alpha^{-2}(1 - \beta + r_K \beta) - r_K], \tag{133}$$

which is a minimum when $\alpha^2 = \beta = (1 + r_K^{1/2})^{-1}$. This value (close to the value of α^2 for minimum energy dissipation by spirals shown in Fig. 12) implies that motions where in most parts of the flagellum the tangent makes an angle with the axis around 40° dissipate least energy for given zero-thrust swimming speed U_0.

By contrast, a minimization of (133) for given flow rate Q involves smaller values of α^2 and β; that is, larger amplitudes of undulation. The difference results almost entirely from the α^{-1} factor in (132), since the logarithmic dependence (105) of K_X on l tends partly to cancel the variation in the $\ln(2l/R)$ factor. If fixing Q does cause U_0 to vary in proportion to α, the rate of working (133) again has a minimum *for given* β when α^2 takes its greatest possible value β (the mean square cosine, β, cannot be less than the square of the mean, α^2). That minimum in turn varies with β in proportion to $1 + r_K \beta (1 - \beta)^{-1}$; this expression decreases towards an asymptote of 1 as β decreases towards zero, implying that the rate of working will be near its minimum for given induced flow when the amplitude of undulations is so large that β, the mean square axial direction cosine of the flagellar tangent, is small.

The theory suggests, then, that whereas undulations of moderate amplitude minimise the rate of working by a flagellum needed to generate a given swimming speed, the minimum needed to generate a given flow near the anterior end of the cell body may be attained for undulations of much larger amplitude. In sessile organisms, undulations of such unusually large amplitude are, in fact, commonly observed (M. A. Sleigh, private communication).

This section, however, has made only a small beginning in the study of flow fields generated by flagella. It will be particularly interesting to investigate in the future what flow fields relevant to the feeding problems of moving organisms may be generated by the opposing action of flagellar thrust and cell body drag (see § 3.4). An extended hydrodynamic theory for flagella with mastigonemes (§ 2.2) is also most desirable and could be used to throw light on several questions relevant to flow patterns with a feeding function.

4. Conclusions. In this Lecture, I first tried to indicate how rich an area of science is the biofluiddynamics of microorganisms with flagella and related organisms; then, in order to suggest what significant contributions can be made to it by a proper application of mathematics, I analyzed in detail certain selected problems of flagellar hydrodynamics. Obviously, the range of biofluiddynamic

phenomena which I briefly surveyed (with references) in § 2 is enormously wider than the limited range of problems which I analyzed in § 3; in making such a wide survey, my aim was to interest fellow applied mathematicians in the possibility of seeking to analyze in a broadly similar manner many other problems in the biofluiddynamics of microorganisms. Now I want to conclude by emphasizing that it is necessary to communicate the conclusions of any such analysis to colleagues (including colleagues in the life sciences) in clear nonmathematical language. Accordingly, I end my lecture by giving that sort of summary of the conclusions of § 3.

The political principle DIVIDE AND RULE applies to the hydrodynamic analysis of flagellar motions (whether they be the undulations of a eukaryotic flagellum or the postulated rotary motions of a bacterial flagellum or bundle). It is important to distinguish between the velocity-generating function of a flagellar motion and its thrust-generating function; especially, because the nature of the interaction with the fluid medium in the exercise of these two functions is quite different. Fortunately, the two functions can be analyzed separately and then the results can be combined (in quite a simple manner) to study any particular problem of interest.

Specifically, we can analyze first (§ 3.2) the *zero-thrust* swimming which the motion of the flagellum *would* generate if the cell body to which it is attached had no hydrodynamic resistance to be overcome. This represents the "natural" swimming brought about by the flagellar motions themselves in the absence of any counterbalancing drag force. Then the velocity-generating function of the flagellar motions must produce its maximum effect: the zero-thrust swimming speed.

Once we know what zero-thrust swimming a particular flagellar motion will produce, we can readily understand the same motion's thrust-generating function. The principle DIVIDE AND RULE means that we must think separately about *zero-thrust swimming* and the *change due to thrusting*, as follows.

Obviously any hydrodynamic drag on the cell body slows down the organism to below the zero-thrust swimming speed. The flagellum is then being held back from going at its full zero-thrust speed; we can say that *relative to that zero-thrust swimming motion, it is drifting backwards.* Now, quite simply; thrust consists of the *resistance opposing that drift backwards*, and the swimming speed adjusts itself (§ 3.4) so that this thrust exactly balances the drag resisting the forward motion of the cell body.

The interaction with the fluid medium involved in the velocity-generating (zero-thrust) function of flagellar motions has these general characteristics:

(i) the associated flow fields are highly localized (see Fig. 18);

(ii) on the flagellum, there is a rather small "cooperation radius" (distance within which different cross sections of the flagellum are pushing fluid with forces nearly equal in magnitude and direction);

(iii) as a consequence, the effective "resistance coefficients" (normal and tangential) take values much larger than the classical values due to Gray and Hancock (1955), although their *ratio* is little changed (conclusions on this matter are summarized at the end of § 3.3; see also Fig. 13);

(iv) although total thrust is zero, the resultant action of the hydrodynamic forces on the flagellum may be a *couple*, tending to rotate the organism at

an angular velocity determined by the balance between this couple and the damping couple resisting rotation of the cell body;

(v) the resulting corkscrew rotation of an attached spiral flagellum modifies its motions in a manner that has to be taken into account in determining its zero-thrust swimming speed (§ 3.2; see also § 2.2);

(vi) it is the zero-thrust swimming characteristics of flagellar motions (see Fig. 12 for data on these in the case of spiral motions) that determine the *rate at which they do work* even in the thrusting case.

By contrast, the interaction with the fluid medium involved in the thrust-generating function of flagellar motions (which is associated with a backward drift *relative to* the zero-thrust swimming velocity) has these general characteristics:

(i) the associated flow fields are on a large scale (Fig. 19);

(ii) there is a large "cooperation radius" of thrusting activity (comparable to the length of the flagellum);

(iii) as a consequence, the total resistance to the abovementioned backward drift (namely, the thrust) can be described by means of a special resistance coefficient (105) *much smaller* than those involved in the determination of zero-thrust swimming;

(iv) thrusting activity makes negligible change to those couples involved in determining the organism's rotation;

(v) neither does it change the rate at which the flagellar motions do work (although it involves a reduction in the swimming speed for the same rate of working).

The simple way in which knowledge of the different characteristics of the interaction of flagellar motions with the fluid medium in the velocity-generating and thrust-generating cases can be combined for the analysis of a particular problem is illustrated in § 3.5 by the study of flow fields generated by flagellar motions in *sessile organisms*. These are stationary relative to the undisturbed fluid; therefore, relative to the zero-thrust swimming speed, they drift backwards *at the zero-thrust swimming speed* itself! Accordingly, they exert a thrust determined, as the resistance opposing that backward drift at the zero-thrust swimming speed, from the use of a resistance coefficient at the *lower* level associated (see above) with a large cooperation radius of thrusting activity.

This thrust, being opposed by an equal and opposite reaction in a stalk attaching the organism to a substrate, does not move the organism. The corresponding reaction on the fluid, however, generates a large-scale flow field (Fig. 19) that can be important for feeding purposes. Interestingly enough, the undulations required to generate a given flow rate with minimum rate of working are of much greater *amplitude* than those characteristic of swimming with minimum rate of working.

Beyond the analyses of §§ 3.2–3.5 that I have briefly summarized above, I see great scope for use of the basic theorem of § 3.1 to study a much broader range of flagellar motions. Evidently, the computational possibilities of using that theorem to determine force distributions associated with a wide variety of flagellar velocity distributions are substantially enhanced, now that first approximations based on much better resistance coefficients than were previously available can be used to initiate an iteration. Those end effects that were neglected in § 3, and many other

effects involving quite different shapes of flagellar motion, may well yield to numerical analysis along these lines. At the same time, it will be most important that such investigation of hydrodynamical interactions is carefully integrated, in the way I have tried to exemplify in this Lecture, with the necessary analysis of the kinematics, and more generally of the mechanics, of the organism's own motion.

REFERENCES

G. K. BATCHELOR (1970), J. Fluid Mech., 44, pp. 419–440.
H. C. BERG (1974), Nature, 249, pp. 77–79.
H. C. BERG AND R. A. ANDERSON (1973), Nature, 245, pp. 380–382.
H. C. BERG AND D. A. BROWN (1972), Nature, 239, pp. 500–504.
J. R. BLAKE (1971), Proc. Cambridge Philos. Soc., 70, pp. 303–310.
J. R. BLAKE AND M. A. SLEIGH (1974), Biol. Revs., 49, pp. 85–125.
J. M. BOUROT (1974), J. Fluid Mech., 65, pp. 513–515.
C. J. BROKAW (1972a), Biophys. J., 12, pp. 564–586.
——— (1972b), Science, 178, pp. 455–462.
V. J. CHAPMAN AND D. J. CHAPMAN (1973), *The Algae*, 2nd ed., Macmillan, New York.
Y. T. CHEN (1950), Quart. J. Microscop. Sci., 91, pp. 279–308.
A. T. CHWANG, H. WINET AND T. Y. WU (1974), J. Mechanochem. and Cell Motility, 3, pp. 69–76.
A. T. CHWANG AND T. Y. WU (1971), Proc. Roy. Soc. Ser. B, 178, pp. 327–346.
A. T. CHWANG, T. Y. WU AND H. WINET (1972), Biophys. J., 12, pp. 1549–1561.
L. R. CLEVELAND AND A. V. GRIMSTONE (1964), Proc. Roy. Soc. Ser. B, 159, pp. 668–685.
R. G. COX (1970), J. Fluid Mech., 44, pp. 791–810.
I. R. GIBBONS (1965), Arch. Biol. Liège, 76, pp. 317–352.
J. GRAY (1968), *Animal Locomotion*, Weidenfeld and Nicholson, London.
J. GRAY AND G. J. HANCOCK (1955), J. Experimental Biol., 32, pp. 802–814.
G. N. HALFEN AND R. W. CASTENHOLZ (1970), Nature, 225, pp. 1163–1165.
G. J. HANCOCK (1953), Proc. Roy. Soc. Ser. A, 217, pp. 96–121.
M. A. HARPER AND J. F. HARPER (1967), Brit. Phycol. Bull., 3, pp. 195–207.
M. E. J. HOLWILL (1966), Physiol. Revs., 46, pp. 696–785.
M. E. J. HOLWILL AND P. D. PETERS (1974), J. Cell Biol., 62, pp. 322–328.
M. E. J. HOLWILL AND M. A. SLEIGH (1967), J. Experimental Biol., 47, pp. 267–276.
L. H. HYMAN (1940), *The Invertebrates: Protozoa through Ctenophora*, McGraw-Hill, New York.
T. L. JAHN AND E. C. BOVEE (1967), *Motile Behaviour in Protozoa*, Research in Protozoology, vol. 1, T. T. Chen, ed., Pergamon Press, New York, pp. 41–200.
T. L. JAHN, W. M. HARRISON AND M. LANDMAN (1963), J. Protozool., 10, pp. 358–363.
V. V. KINGSLEY AND J. F. M. HOENIGER (1973), Bacteriol. Rev., 37, pp. 479–521.
S. H. LARSEN, R. W. READER, E. N. KORT, W. W. TSO AND J. ADLER (1974), Nature, 249, pp. 74–77.
G. F. LEEDALE (1967), *Euglenoid Flagellates*, Prentice-Hall, Englewood Cliffs, N.J.
M. J. LIGHTHILL (1975), *Mathematical Biofluiddynamics*, Society for Industrial and Applied Mathematics, Philadelphia.
H. MACHEMER (1972), Acta Protozool., 11, pp. 295–300.
D. L. MACKINNON AND R. S. J. HAWES (1961), *Protozoa*, Oxford University Press, London.
R. MACNAB AND D. E. KOSHLAND (1974), J. Molecular Biol., 84, pp. 399–406.
M. PARKE AND D. G. RAYNS (1964), J. Marine Biol. Assoc. U.K., 44, pp. 209–217.
O. PIRONNEAU (1973), J. Fluid Mech., 59, pp. 117–128.
D. L. RINGO (1967), J. Ultrastruct. Res., 17, pp. 266–277.
A. J. SALLE (1961), *Fundamental Principles of Bacteriology*, McGraw-Hill, New York.
P. SATIR (1968), J. Cell Biol., 39, pp. 77–94.
W. R. SCHNEIDER AND R. N. DOETSCH (1974), J. Bacteriol., 117, pp. 696–701.
M. SILVERMAN AND M. SIMON (1974), Nature, 249, pp. 73–74.
U. B. SLAYTR AND A. M. GLAUERT (1973), Nature, 241, pp. 542–543.
M. A. SLEIGH (1973), *Biology of Protozoa*, Edward Arnold, London.

M. A. SLEIGH (1974), *Cilia and Flagella*, Academic Press, London.
G. M. SMITH (1955), *Cryptogamic Botany*, 2nd ed., vol. 1, McGraw-Hill, New York.
R. W. SMITH AND H. KOFFLER (1971), Adv. Microbiol. Physiol., 6, pp. 219–339.
K. SUMMERS (1974), J. Cell Biol., 60, pp. 321–324.
K. SUMMERS AND I. R. GIBBONS (1971), Proc. Nat. Acad. Sci. U.S.A., 68, pp. 3092–3096.
B. L. TAYLOR AND D. E. KOSHLAND (1974), J. Bacteriol., 119, pp. 640–642.
C. Y. WANG AND T. L. JAHN (1972), J. Theor. Biol., 36, pp. 53–60.
F. D. WARNER (1970), J. Cell Biol., 47, pp. 159–182.
F. D. WARNER AND P. SATIR (1973), J. Cell Sci., 12, pp. 313–326.
——— (1974), J. Cell Biol., 63, pp. 35–63.
C. WEIBULL (1960), *Movement*, The Bacteria, vol. 1, I. C. Gunsalus and R. Y. Stanier, eds., Academic Press, New York, pp. 153–206.